Department of Materials Science, Faculty of Metallurgy, Technical University of Košice, Slovak Republic

Videoextensometry – non contact technique for strain measurement on the surface and the application in materials research

Ladislav **Pešek**

Principles

Accuracy

Deformation maps

Strain Homo/Heterogeneity

Crack growth resistance: thinn sheets (1-2 mm), CT,

rolling direction, plastic hinge position, loading rate,

CTOD- and J- Δa curve

Other fields of application

Metódy stanovenia deformácií

-Analytické (nutný matematický model)

-Iteračné MKP (nutné poznať vstupné materiálové parametre)

problém = verifikácia

= nelineárne riešenie pre plastické deformácie

-Experimentálne ... Odporová tenzometria, fotoelasticimetria, Moiré, RTG, ...

Videoextenzometria

problém = rozsah použitia: elastická, plastická oblasť

Non contact displacement measuring techniques

- Classical methods restrictions:

- Temperature, field of view, mass

- FEM relations between σ and ε

- Systems:

- CCD , CMOS camera + PC

- frame graber (analog signal $\rightarrow$ digitized)

- software (surface images loading and processing)

- Non contact
- New experimental technique
- Measuring on the surface
- More principles of non contact displacement measuring

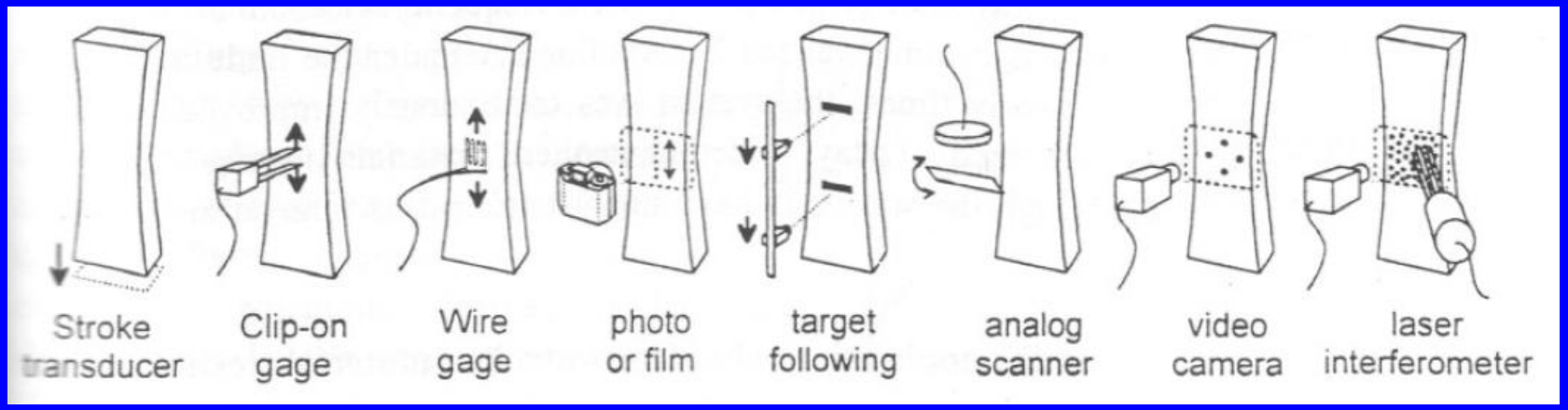

G'Sell, C. Hiver, J.: Video-Controlled Materials Testing and In-Situ Microstructural Characterization, Nancy (INPL), 1999, 16 - 18 November

ESPI

Electronic speckle pattern interferometry

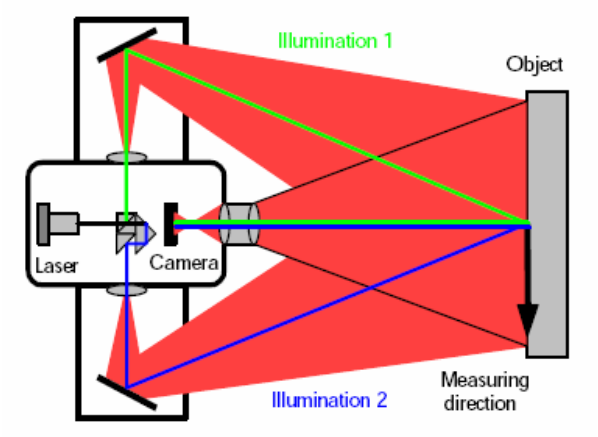

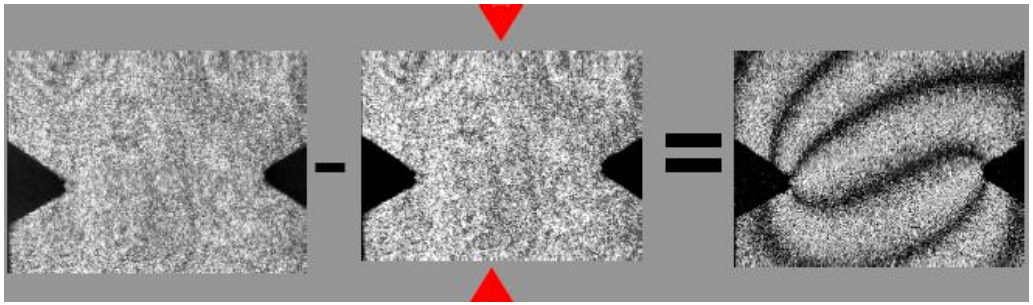

Reference image – deformed image

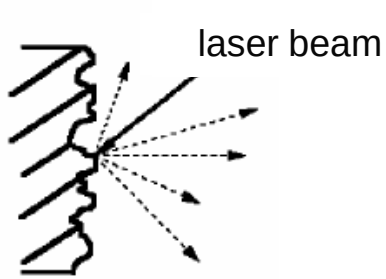

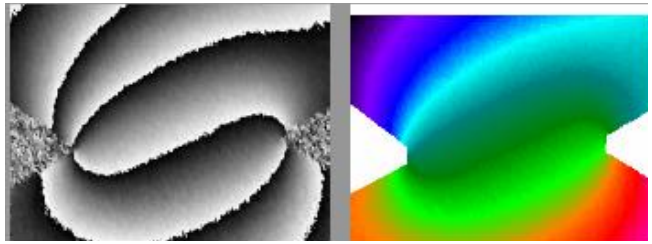

displacement field

DIC

Digital image correlation

- subsets similarity
- normalized coeficient of cross correlation

$$r = \frac{\sum_{i=1}^{n}\sum_{j=1}^{n} I_1(x_i, y_i) I_2(x_i + u, y_i + v)}{\sum_{i=1}^{n}\sum_{j=1}^{n} \sqrt{I_1^2(x_i, y_i)}\sqrt{I_2^2(x_i + u, y_i + v)}}$$

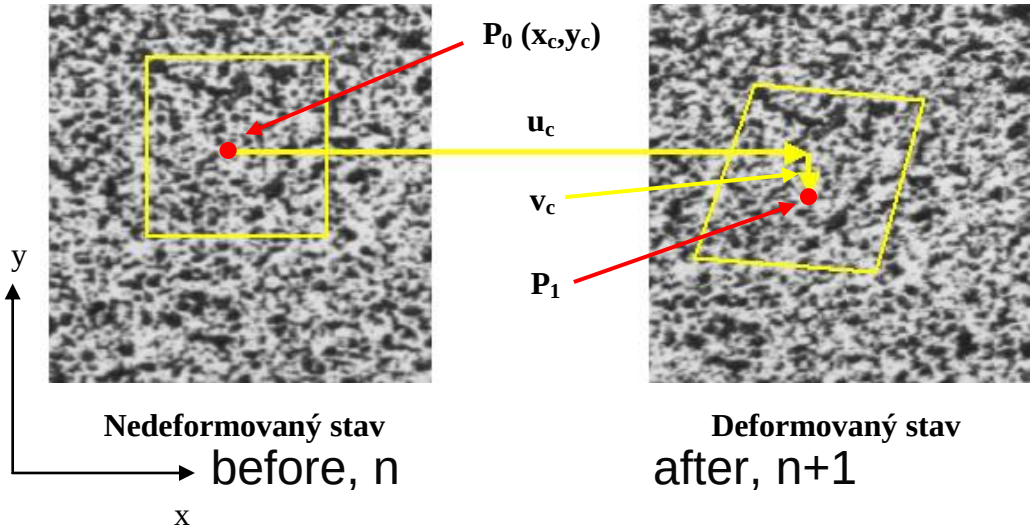

Treshold technique

image → binary image - optimized gray scale

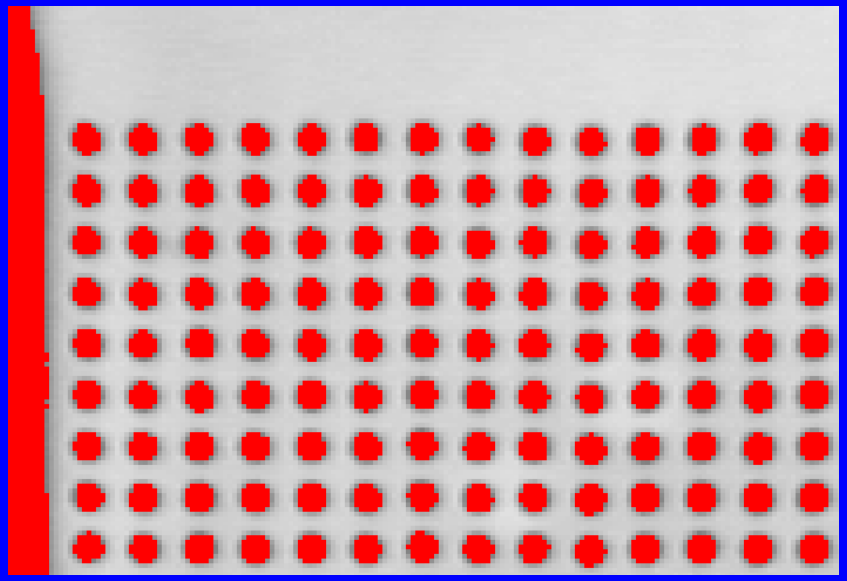

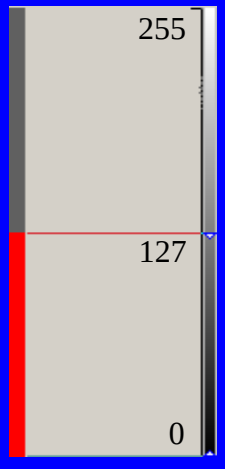

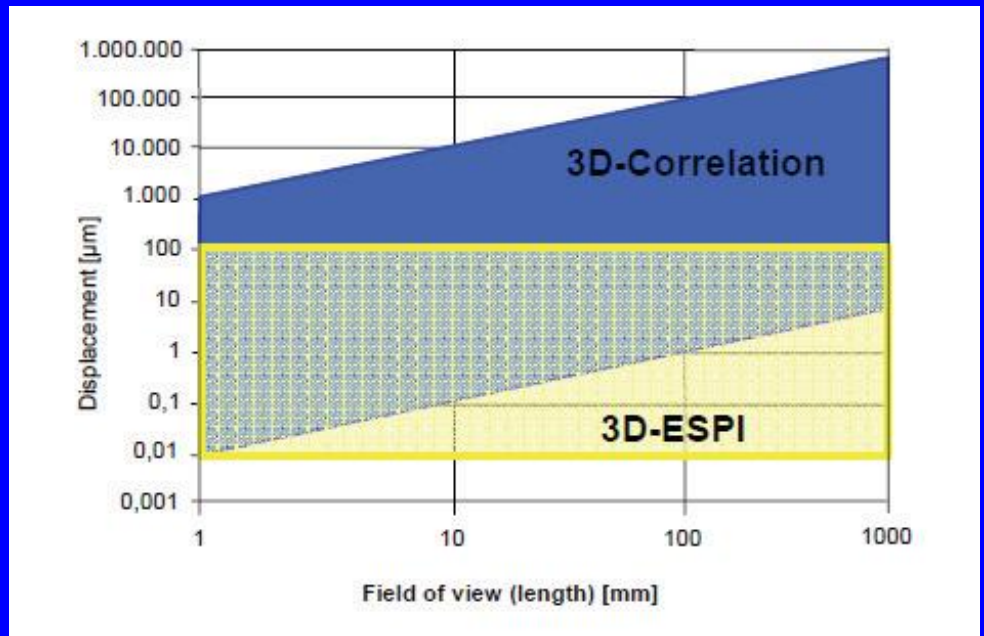

Videoextenzometer ME 46

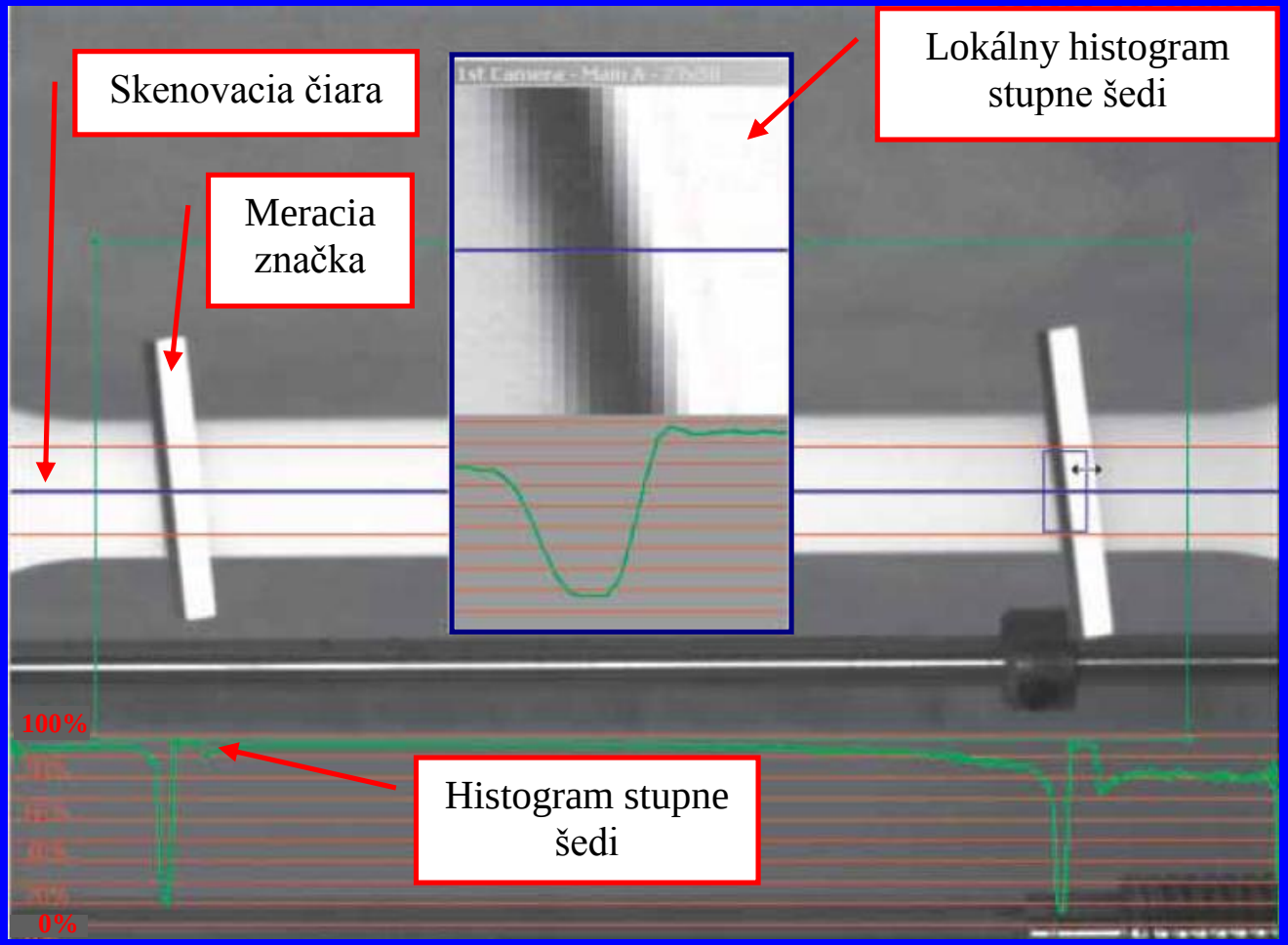

Videoextensometer ME 46

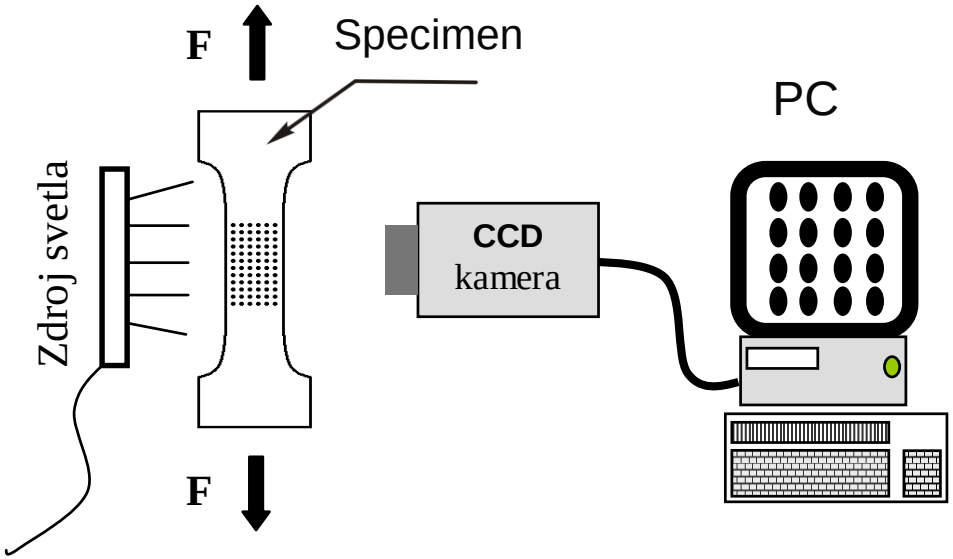

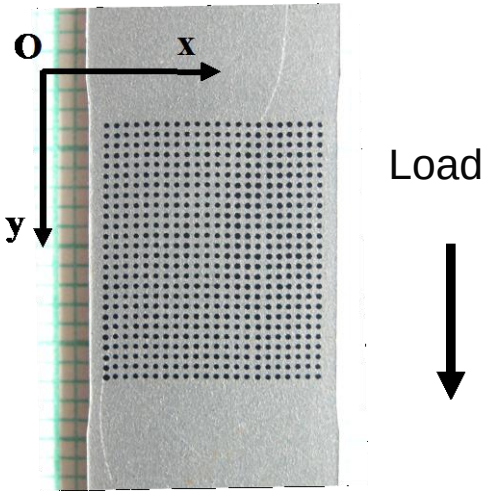

Videoextensometry

Experimental set-up

Accuracy
1 – 2 %

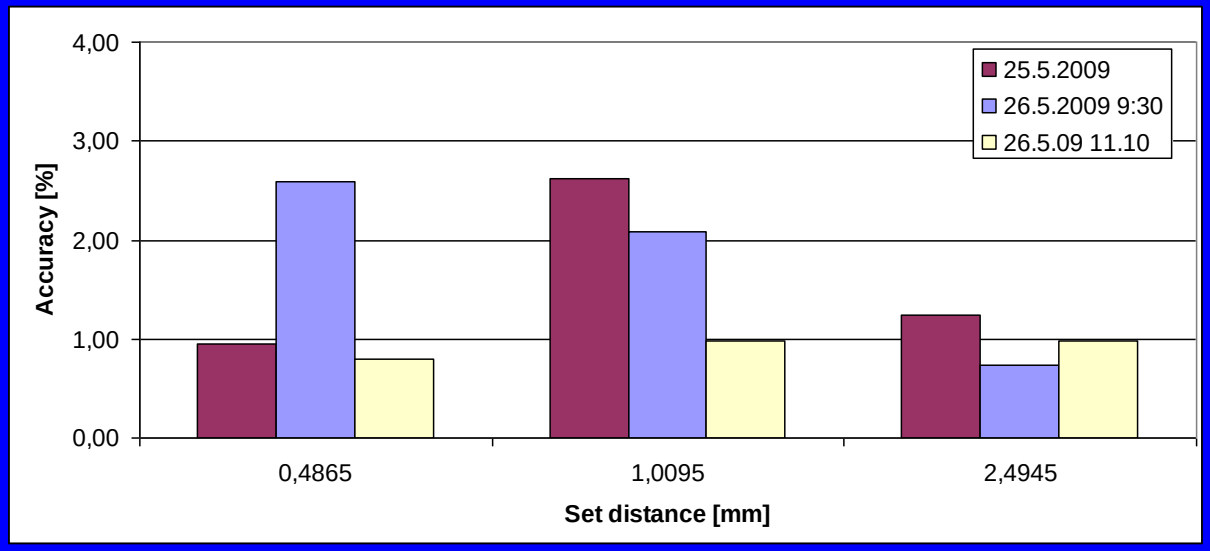

Videoextensometry

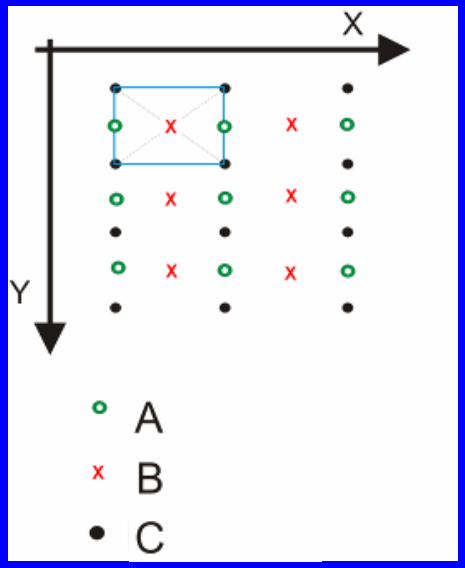

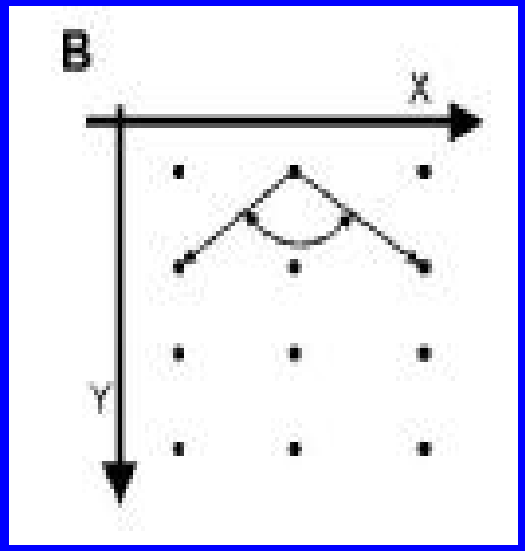

$$d\varepsilon_x = \frac{\partial(du_x)}{\partial x}$$

$$d\varepsilon_y = \frac{\partial(du_y)}{\partial y}$$

Strain homogeneity

ε_z if small thickness

True stress $\sigma = R(1 + \varepsilon_L)$

Strain rate $d\varepsilon/dt$

Strain gradients $d\varepsilon/dx$

Strain

- logarithmic strain tensor:

$\boldsymbol{\varepsilon}^{\log} = \frac{1}{2}\ln(\mathbf{F}\mathbf{F}^{T})$

$$\mathbf{F} = \begin{pmatrix} 1+\frac{\partial u}{\partial x} & \frac{\partial u}{\partial y} & \frac{\partial u}{\partial z} \\ \frac{\partial v}{\partial x} & 1+\frac{\partial v}{\partial y} & \frac{\partial v}{\partial z} \\ \frac{\partial w}{\partial x} & \frac{\partial w}{\partial y} & 1+\frac{\partial w}{\partial z} \end{pmatrix}$$

- logarithmic equivalent strain

$$\varepsilon_{eq}^{\log} = \sqrt{\frac{2}{3}((\varepsilon_{xx}^{\log})^2 + (\varepsilon_{yy}^{\log})^2 + (\varepsilon_{zz}^{\log})^2 + 2(\varepsilon_{xy}^{\log})^2)}$$

Videoextensometry

A - distance, B - element, C – node (dot)

	ε_x [%]	ε_y [%]
A	29.4	155.1
B	27.9	153.2
C	29.03	137.2

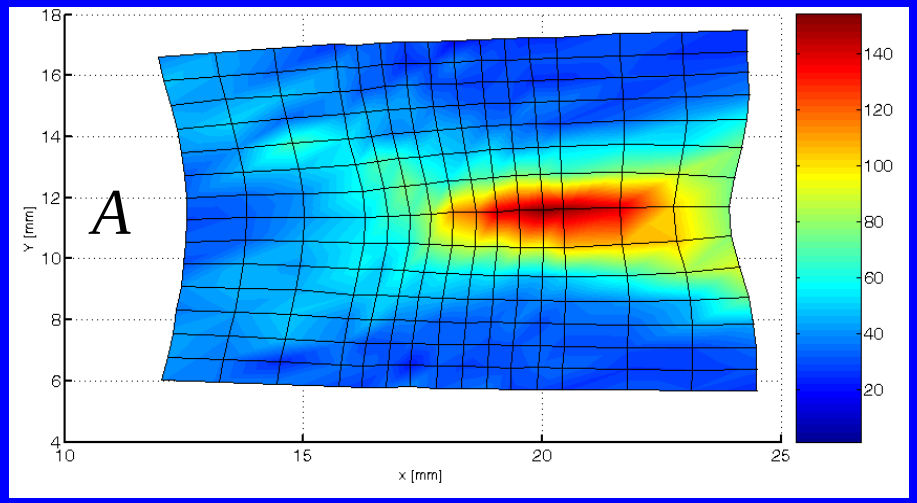

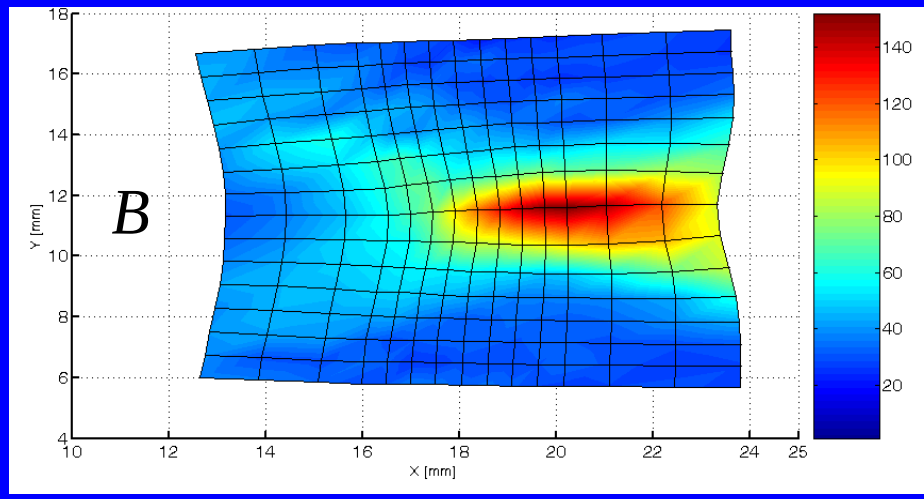

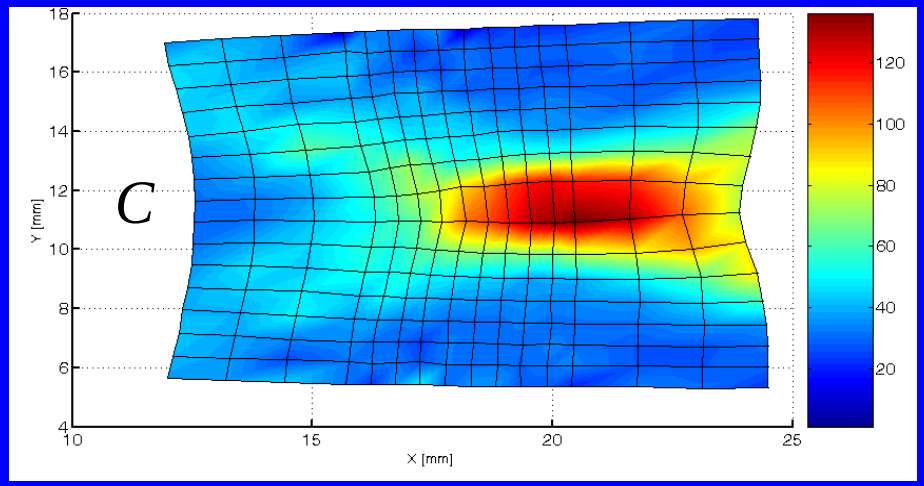

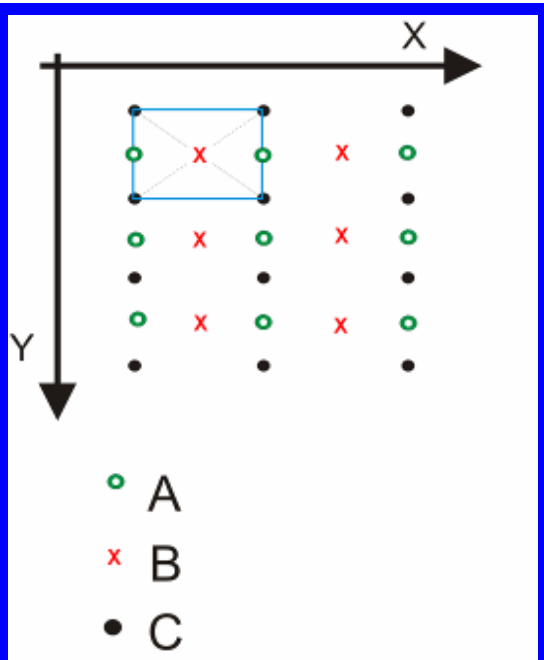

Strain gradient I

Displacement field without smoothing

bicubic plates

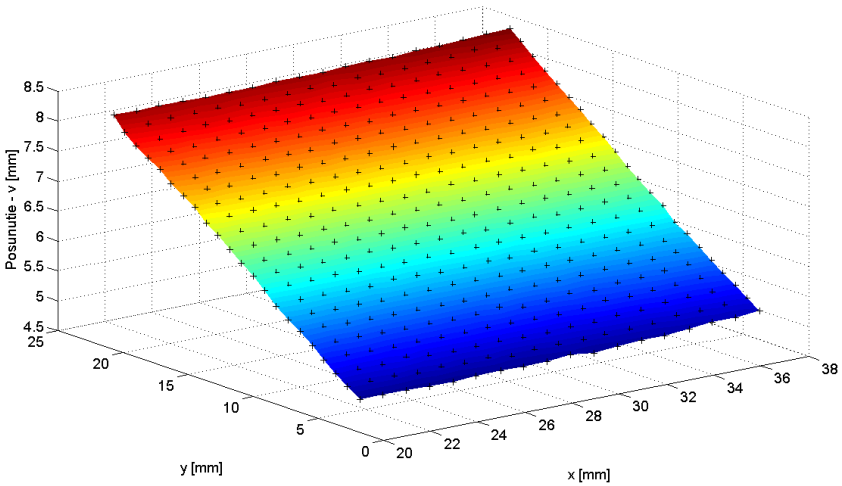

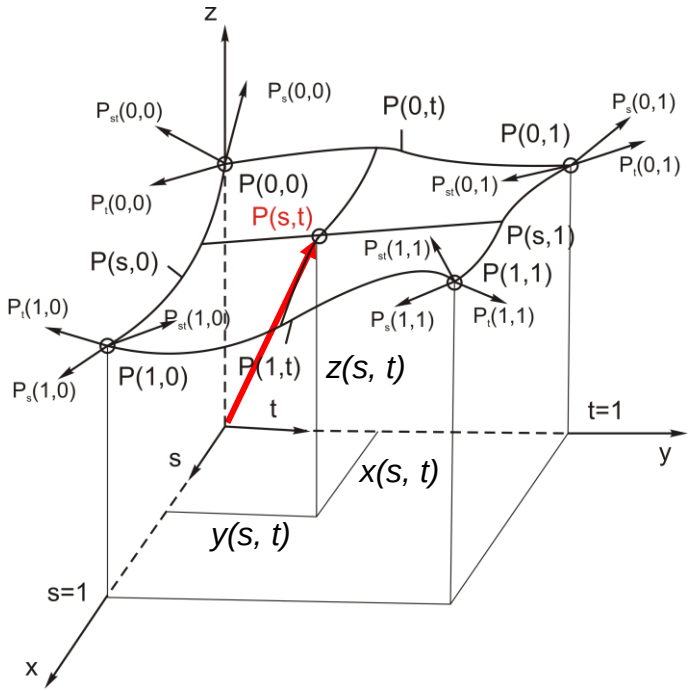

Strain gradient II

Displacement field with smoothing

thin plate splines

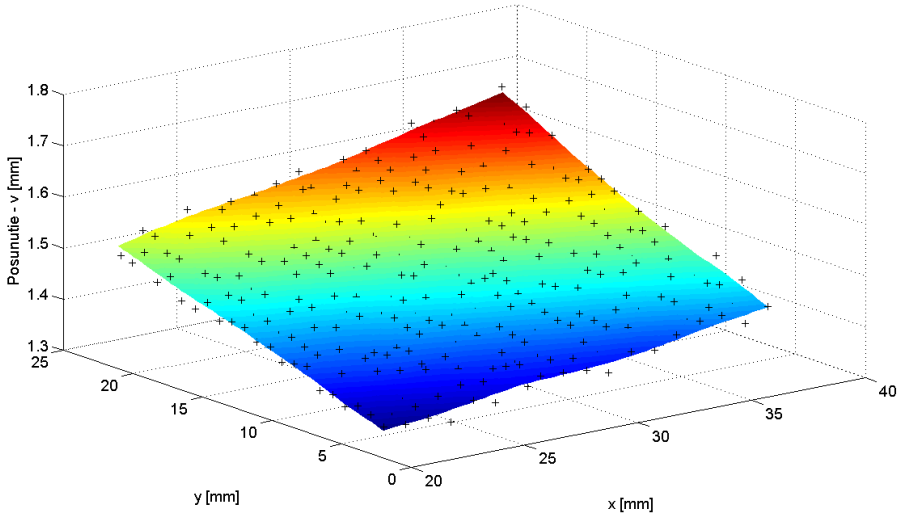

Strain gradient

$$gradf = \nabla f = \frac{\partial f}{\partial x}\vec{i} + \frac{\partial f}{\partial y}\vec{j}$$

IF steel, perforation

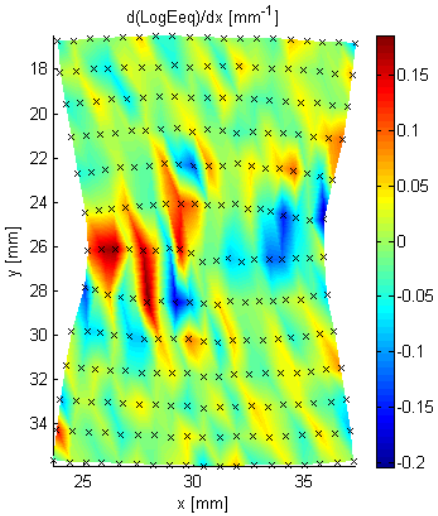

Gradient *x*

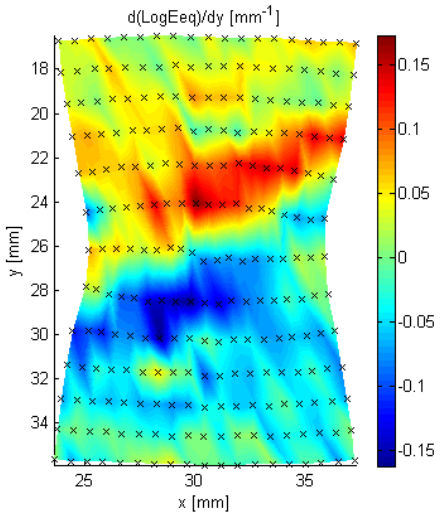

Gradient y

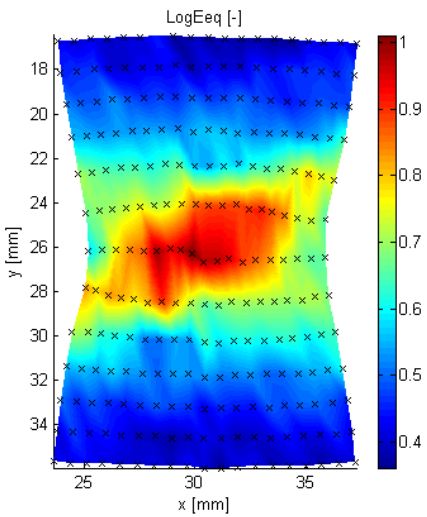

Oceľ IF, deformačný stav - perforácia

Deformation (strain) maps

IF steel

strain localisation

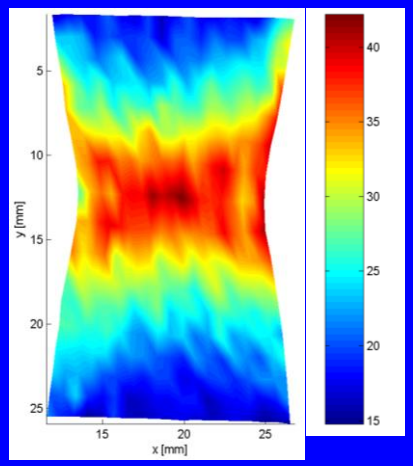

(a) ε_T [%]

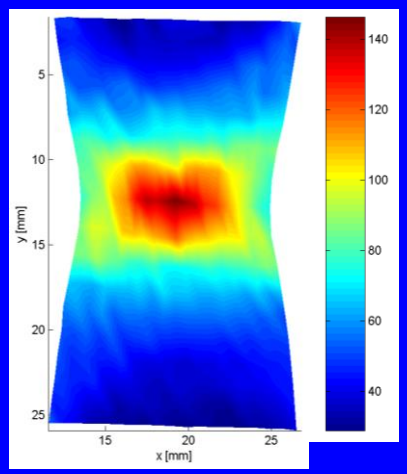

(b) ε_L [%]

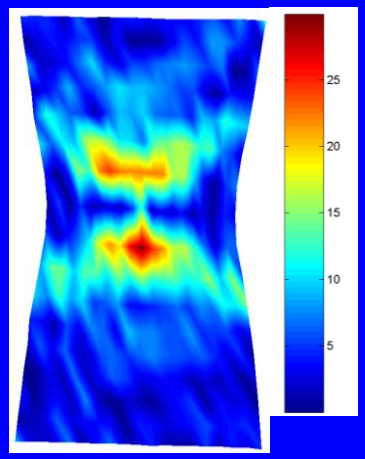

(c) **GY** [%/mm]

TRIP steel

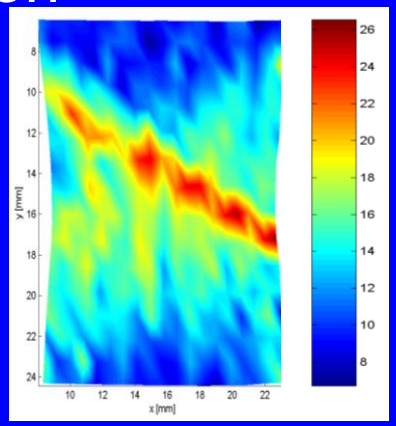

(a) ε_T [%]

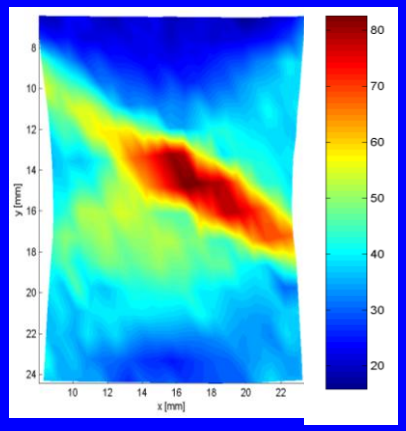

(b) ε_L [%]

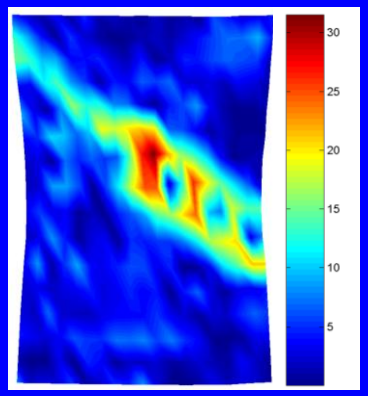

(c) **GY** [%/mm]

Strain maps

Strain

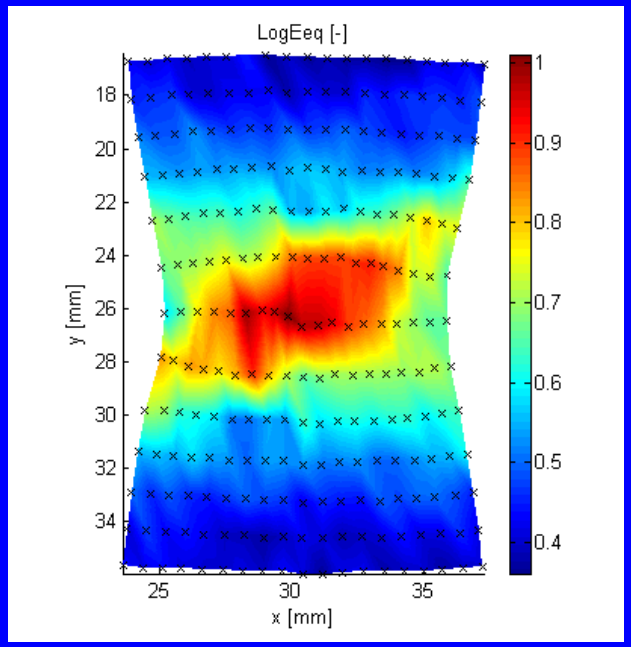

Strain gradient

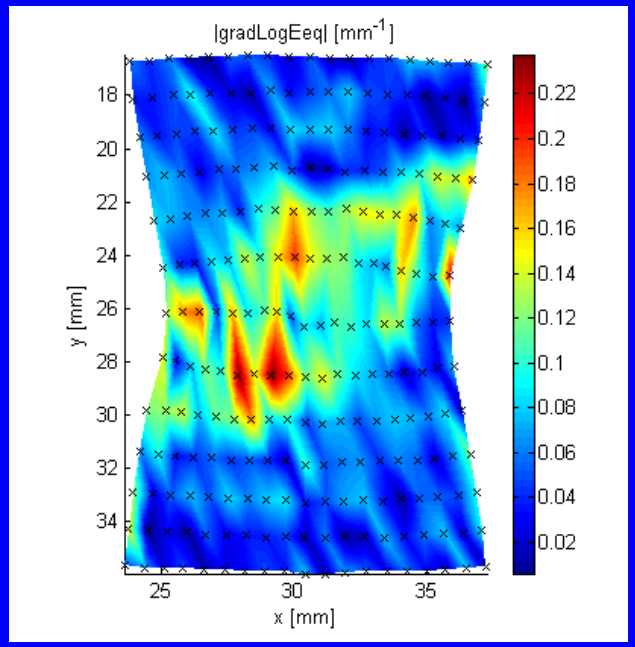

Vector map

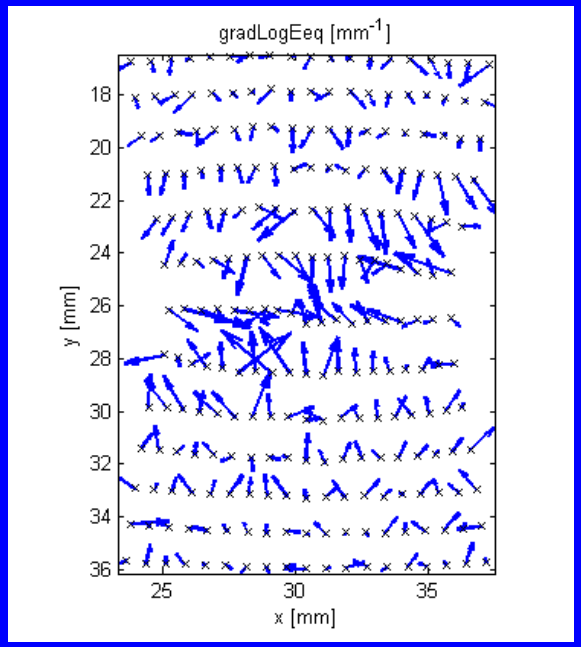

Strain rate

logarithmic equivalent strain

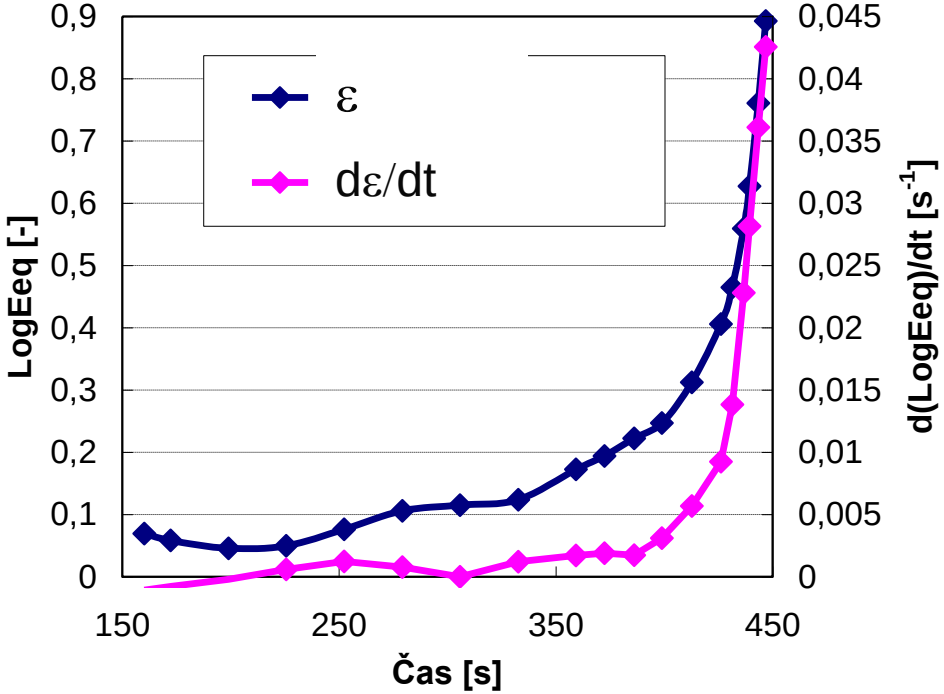

Zeit

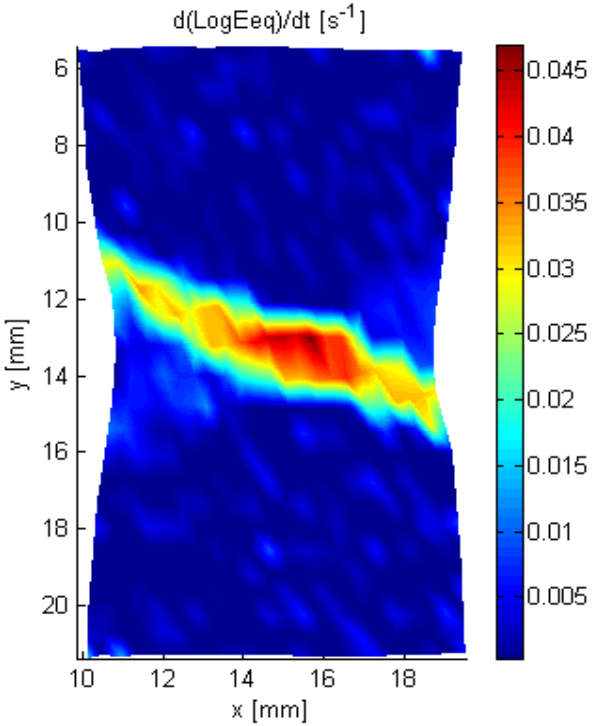

Thickness - comparison

DP steel, thickness after fracture

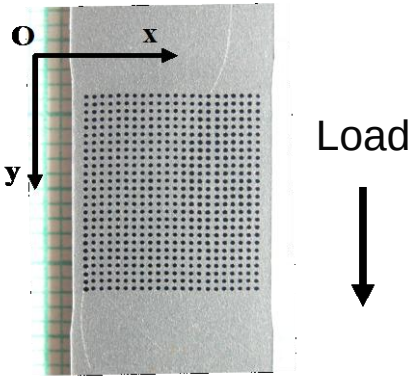

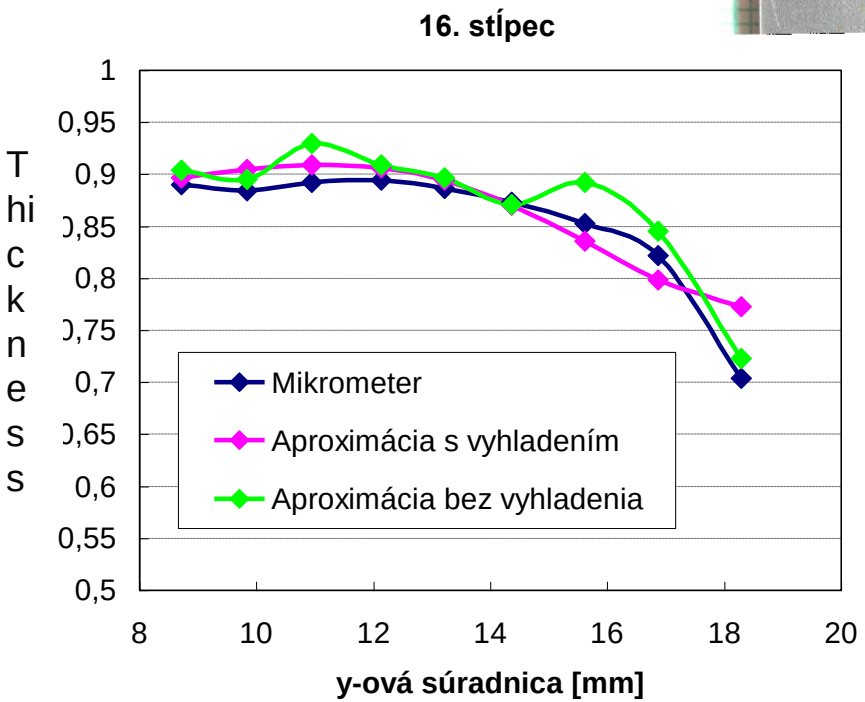

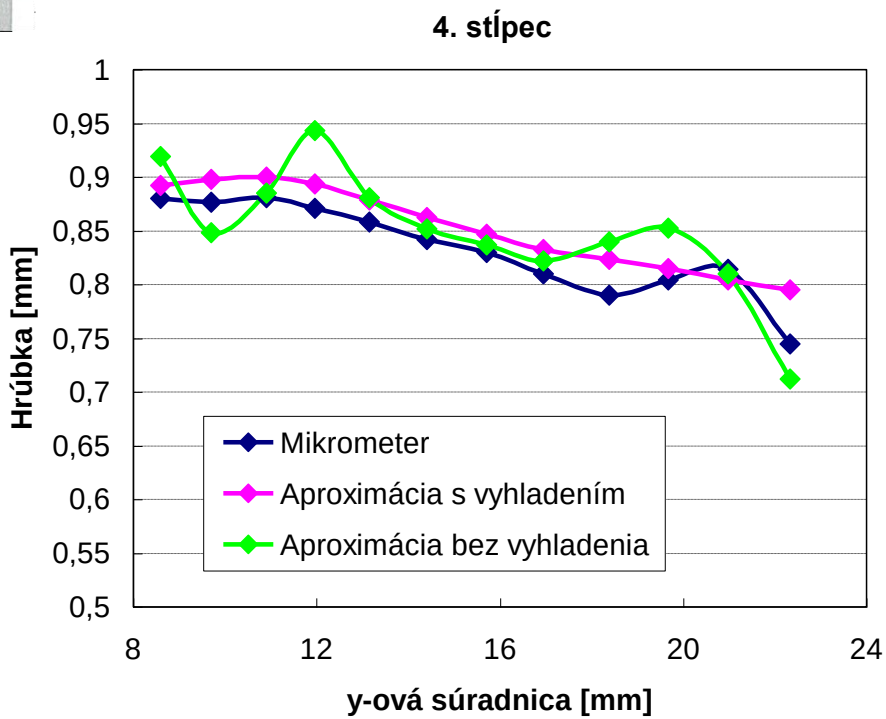

Strain homo/heterogeneity - uniform strain

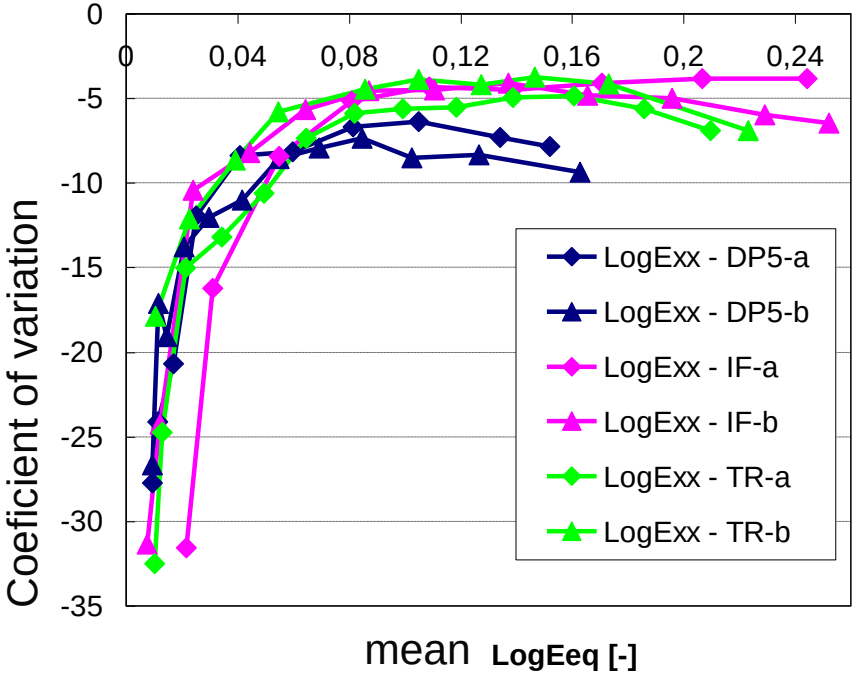

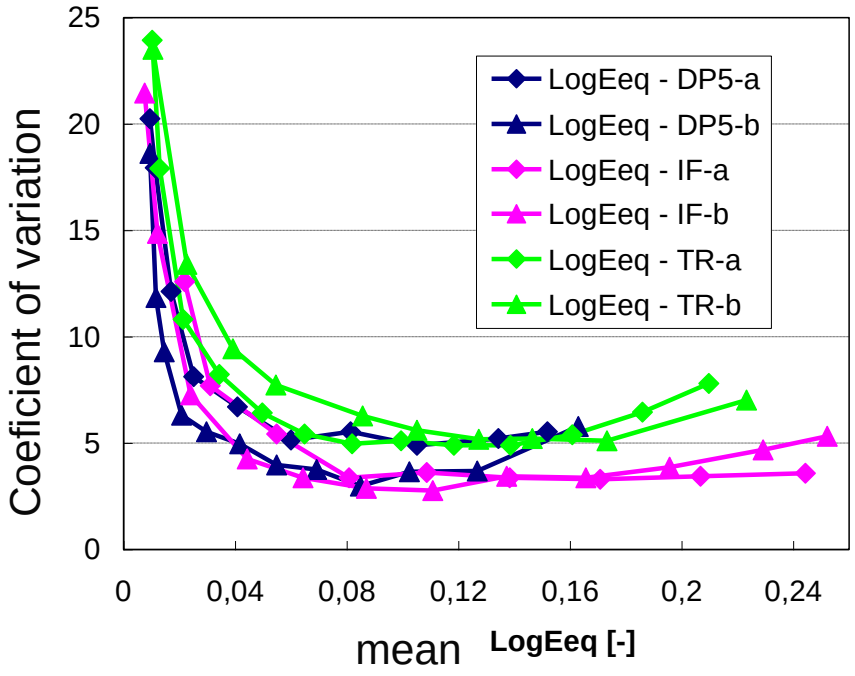

Strain localization
DP500 and IF steel

Based on dε/dt

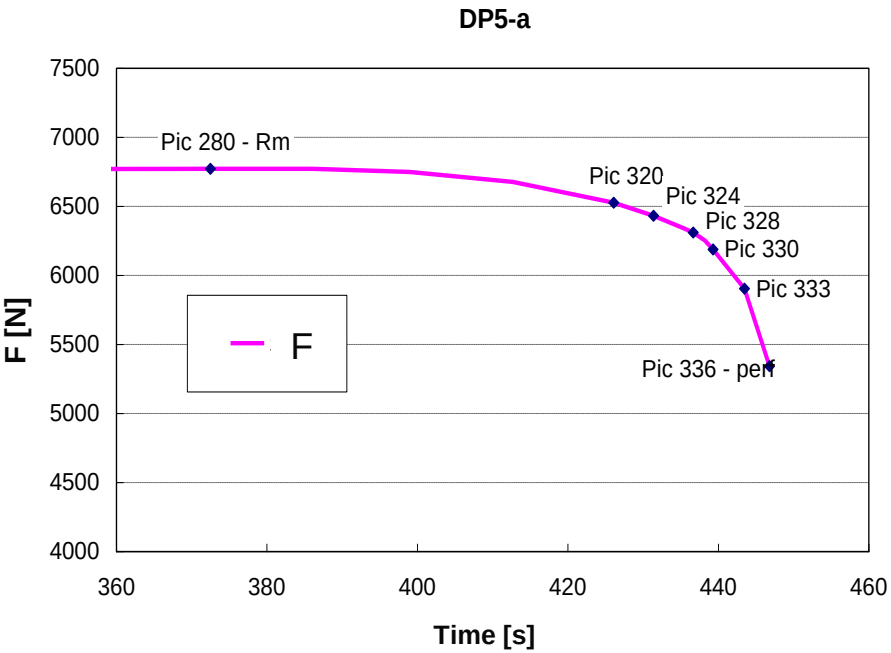

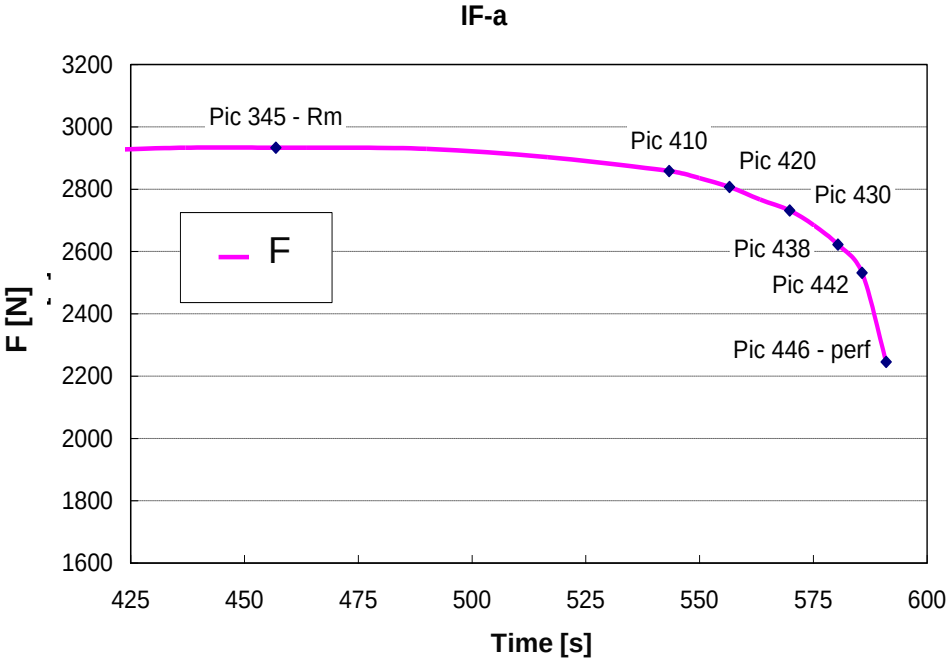

Strain localization

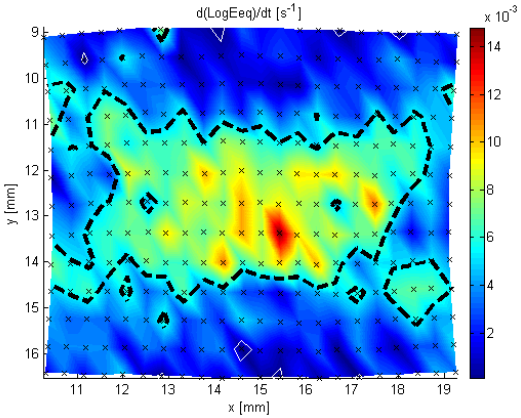

DP-a Pic 320

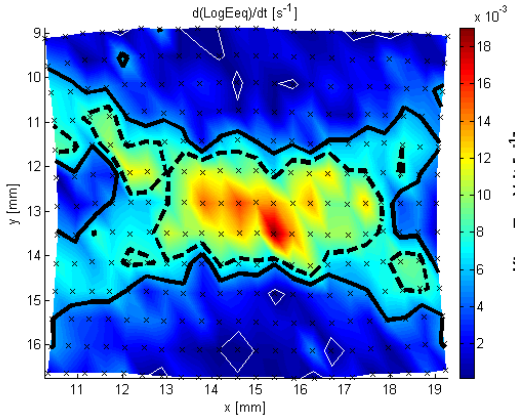

Pic 324

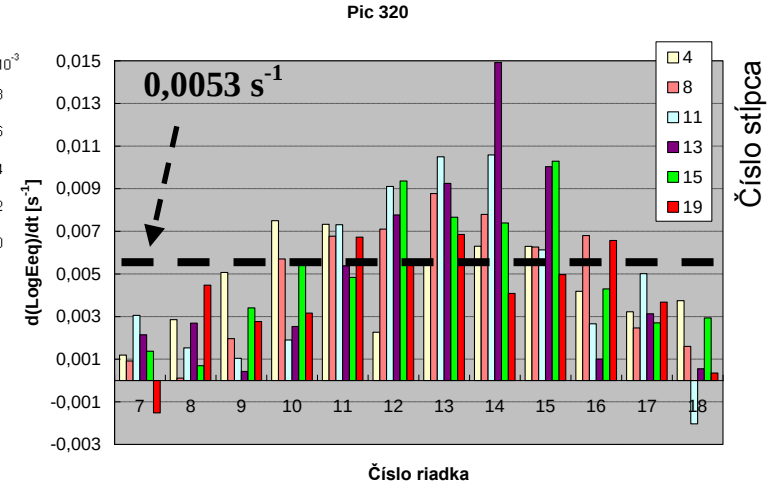

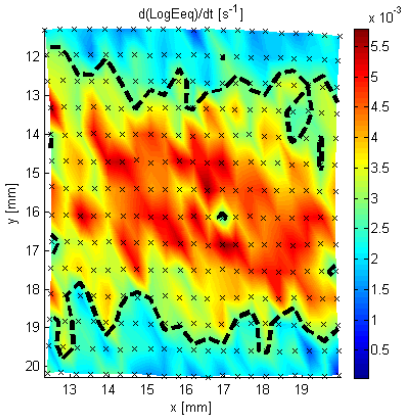

IF-a Pic 410

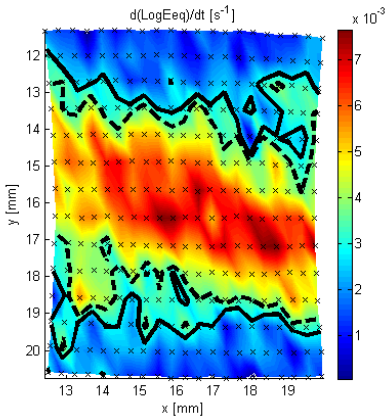

Pic 420

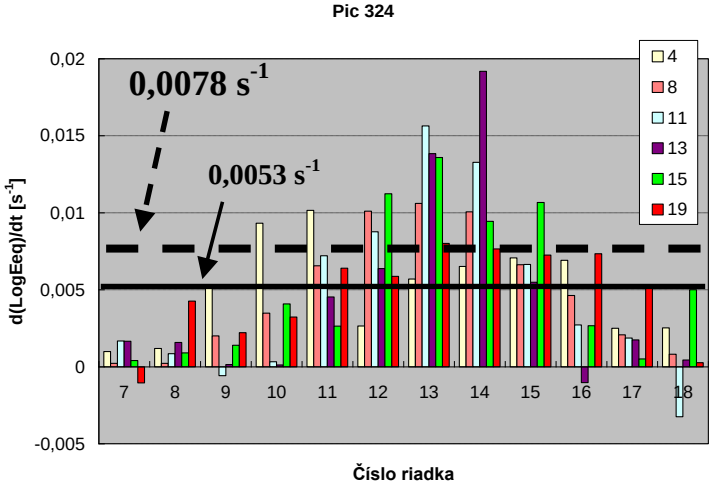

Strain localization

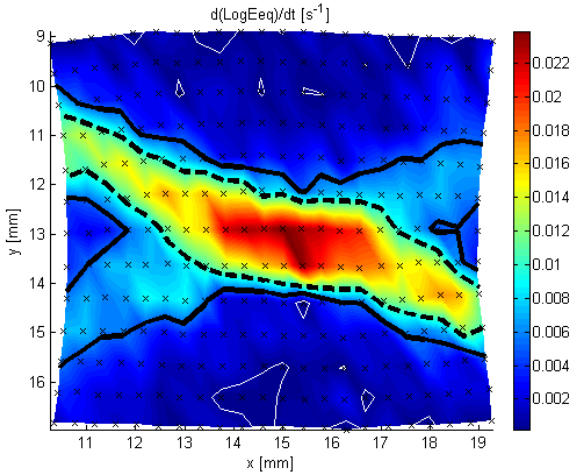

DP-a Pic 328

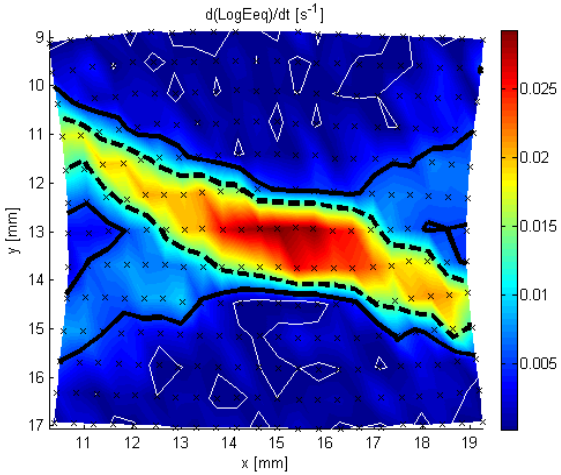

Pic 330

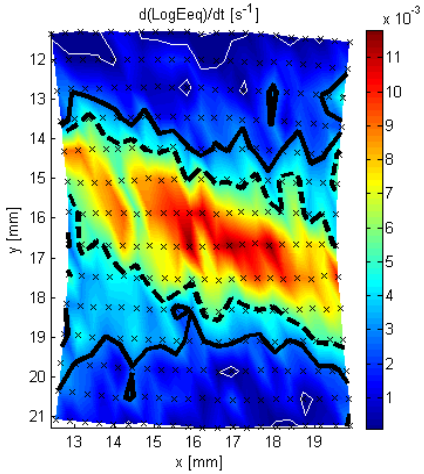

IF-a Pic 430

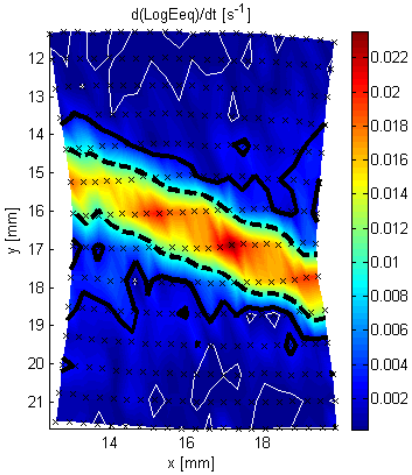

Pic 438

Strain localization

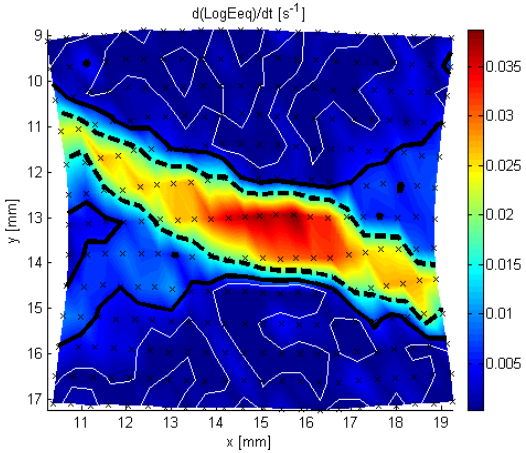

DP-a Pic 333

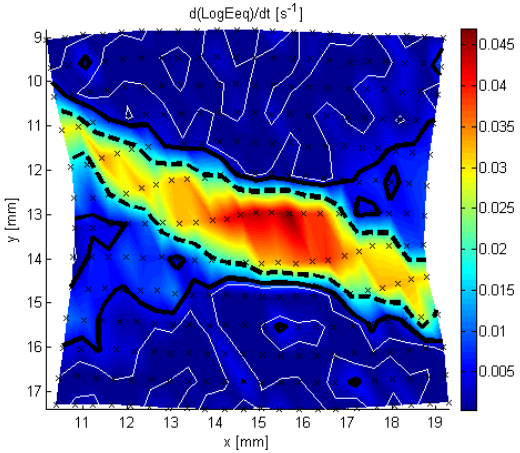

Pic 336 - perf

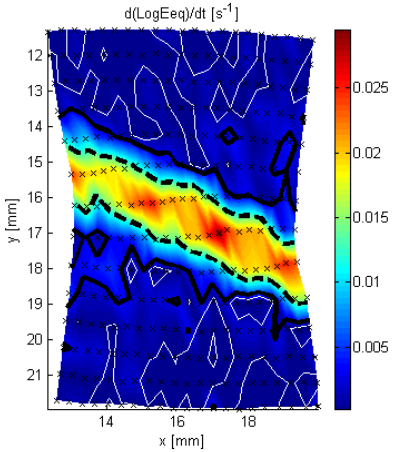

IF-a Pic 442

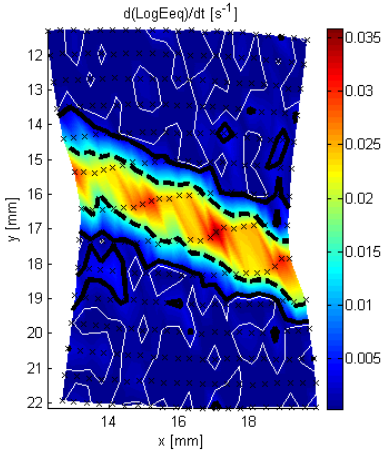

Pic 446 - perf

Slip band - perforation

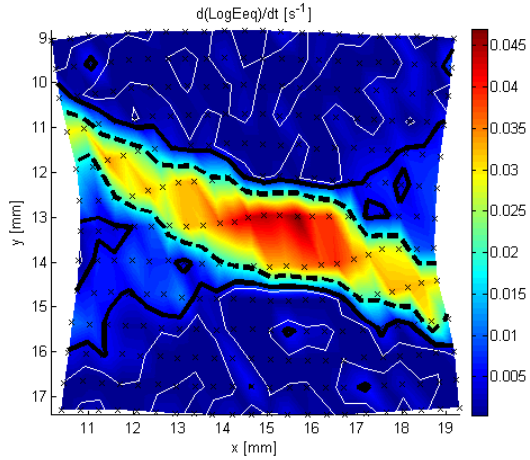

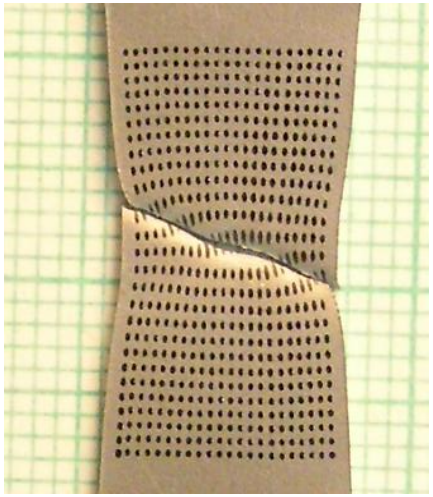

DP-a Pic 336 - perf

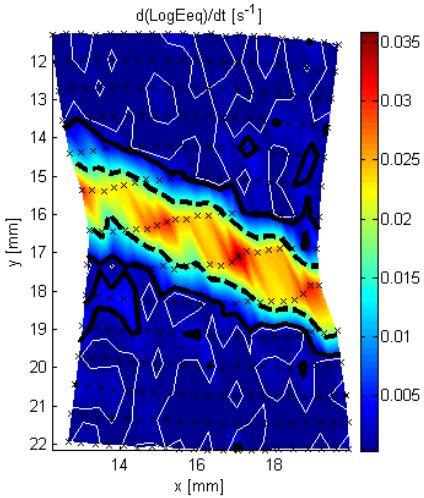

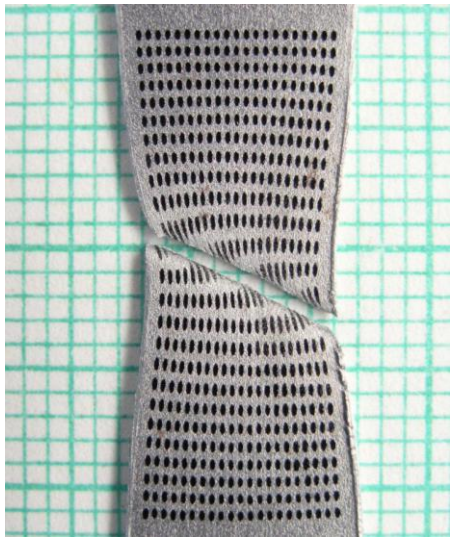

IF-a Pic 446 - perf

Strain localization before perforation

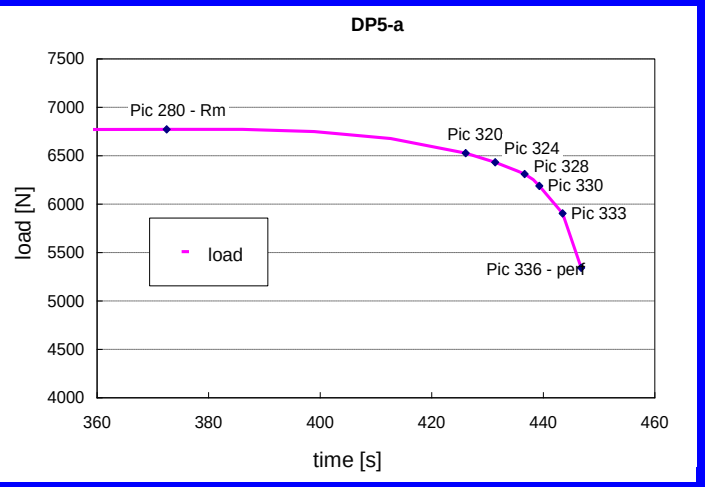

DP, Pic 320

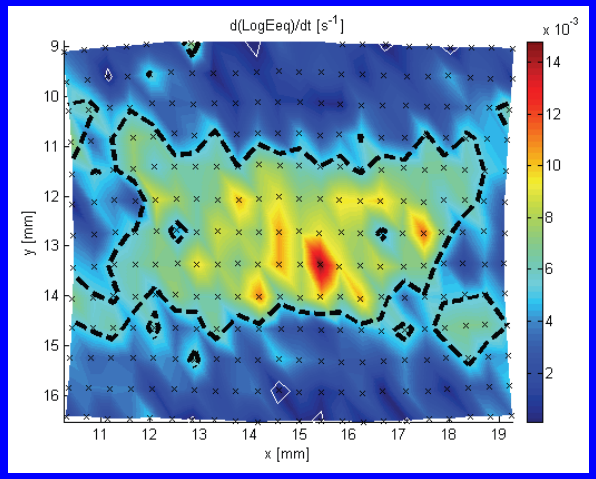

DP, Pic 324

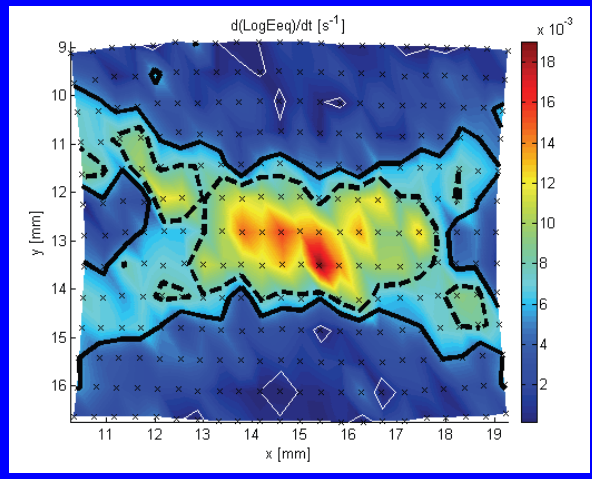

DP, Pic 330

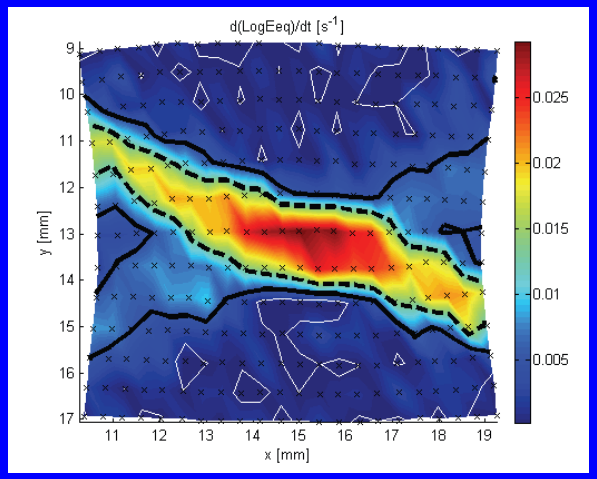

DP, Pic 333

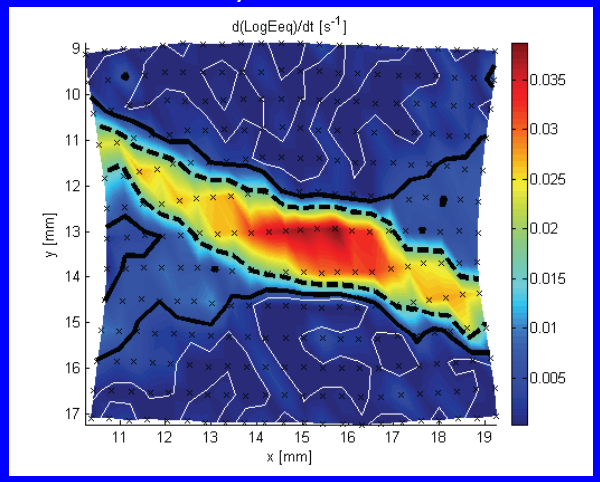

DP, Pic 336- perf

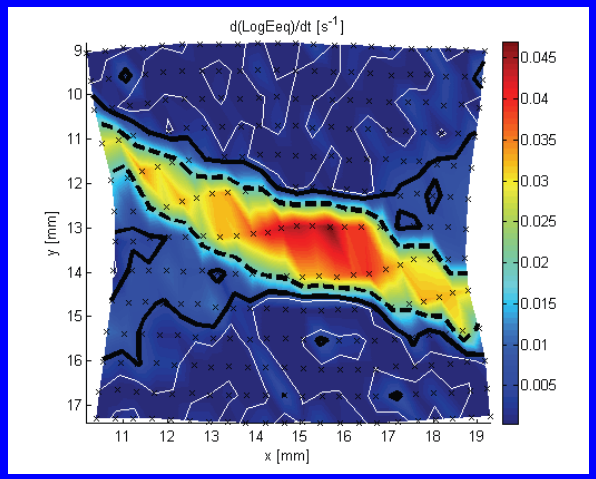

Consumption of energy

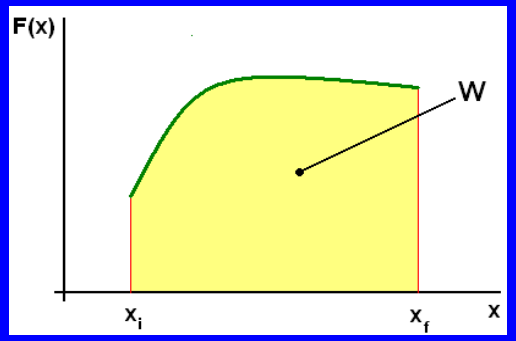

- **Plastic deformation**
- **Stable crack growth (when occurs)**
- **Elastic deformation (reversible)**

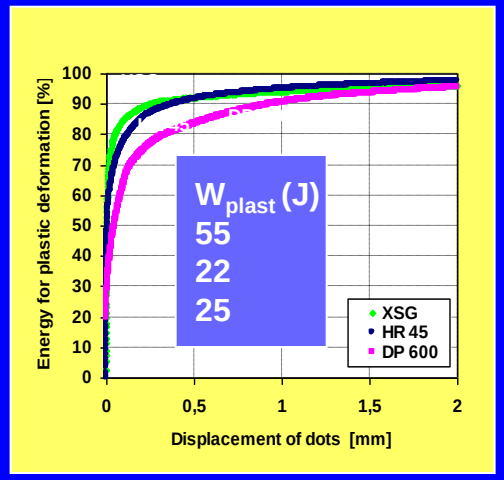

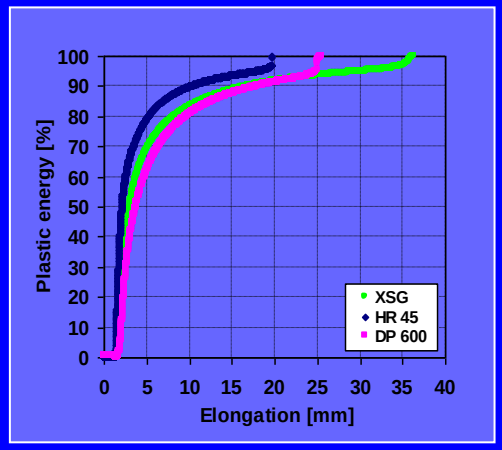

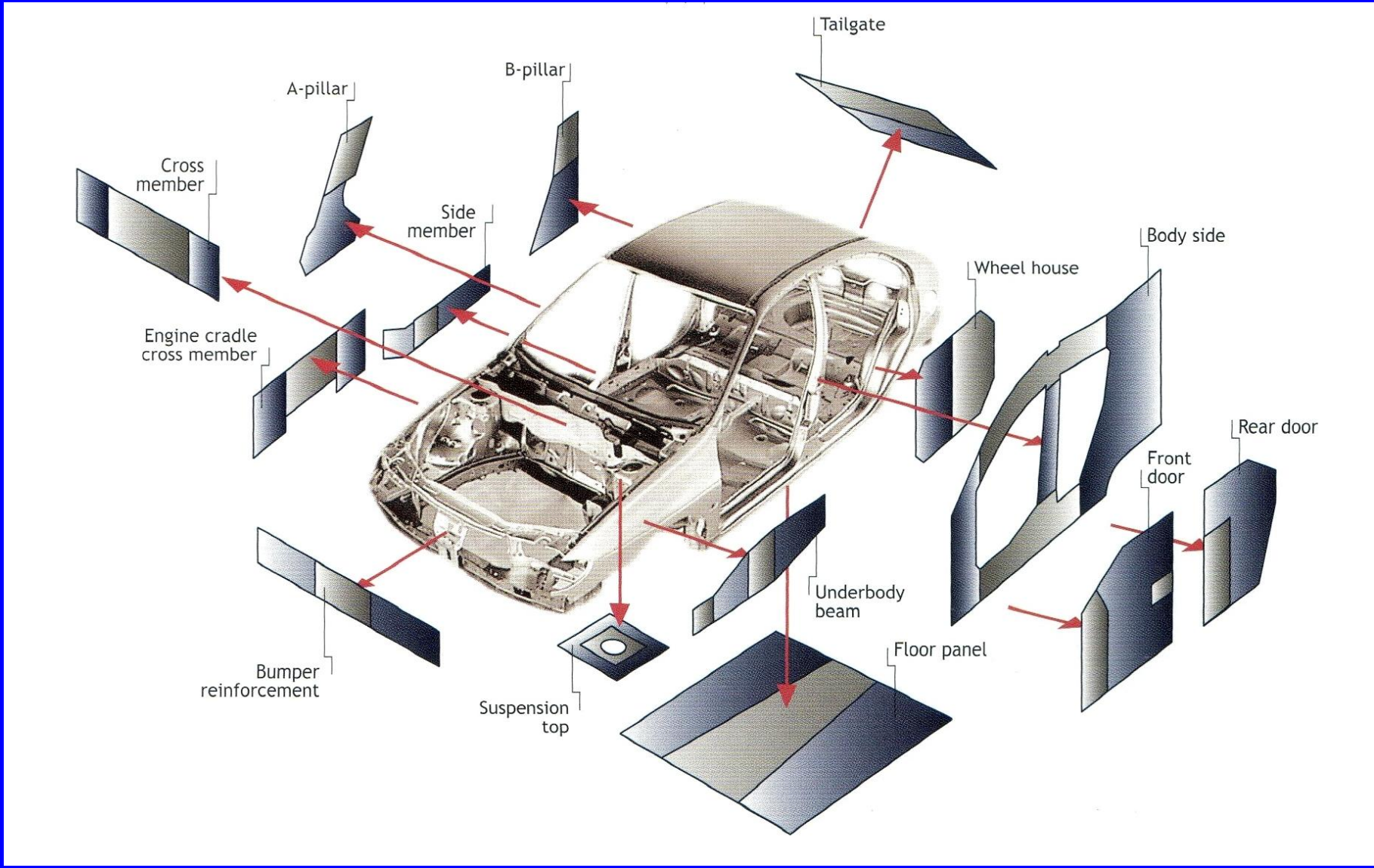
Tailgate
B-pillar
A-pillar
Cross member
Side member
Body side
Wheel house
Engine cradle cross member
Rear door
Front door
Underbody beam
Floor panel
Bumper reinforcement
Suspension top

Investigated material

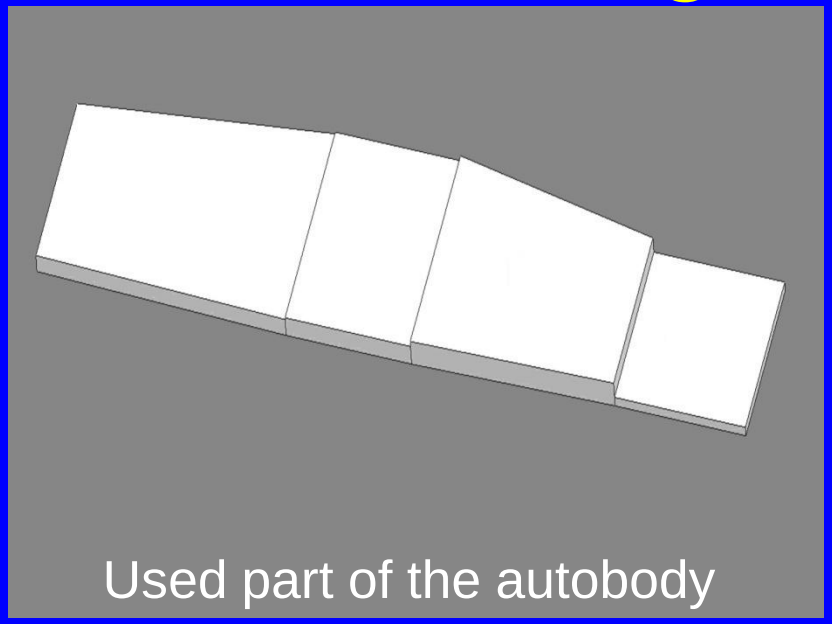

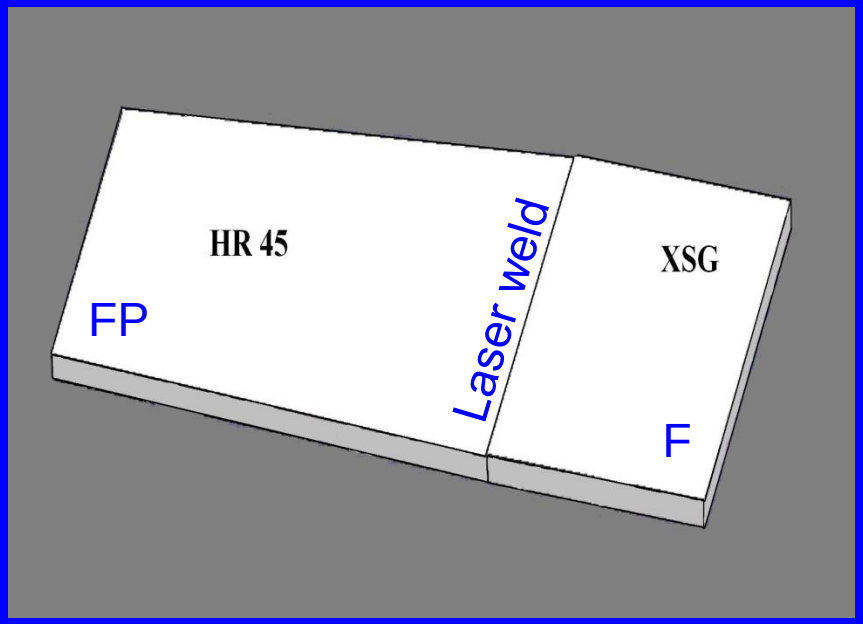

Steel	R_e [MPa]	R_m [MPa]	A [%]	Thickness [mm]
F (IF)	182	300	45	1.95
FP	382	493	25	1.8
DP	357	580	25	1.6

CT specimen

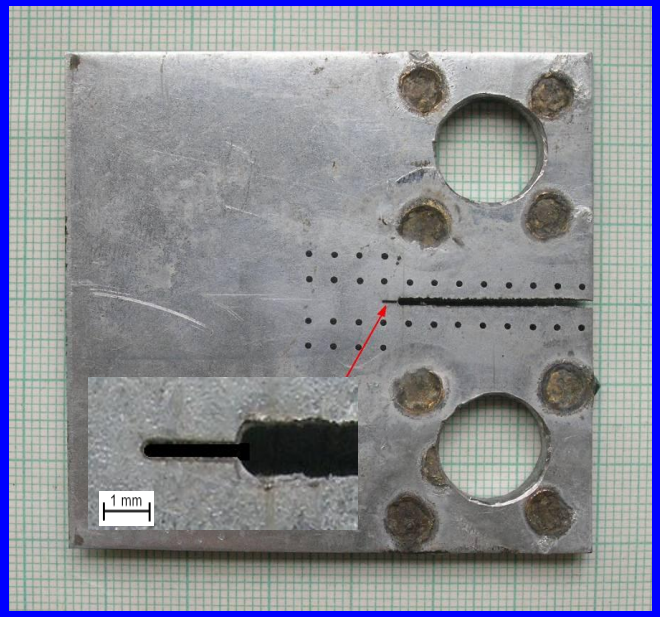

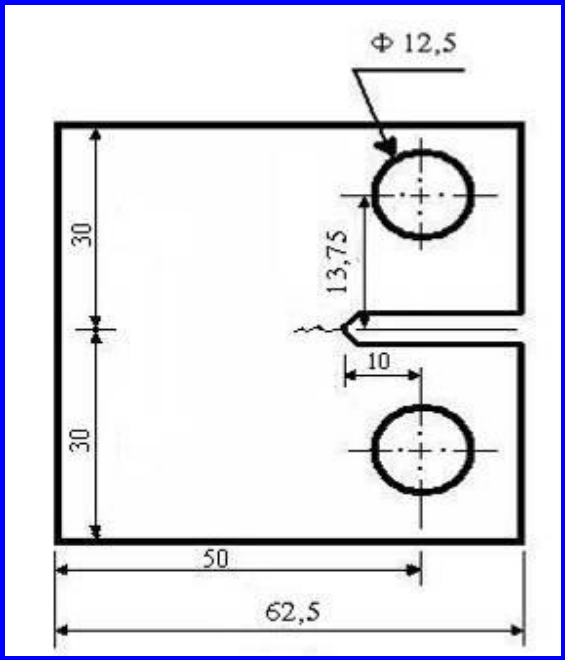

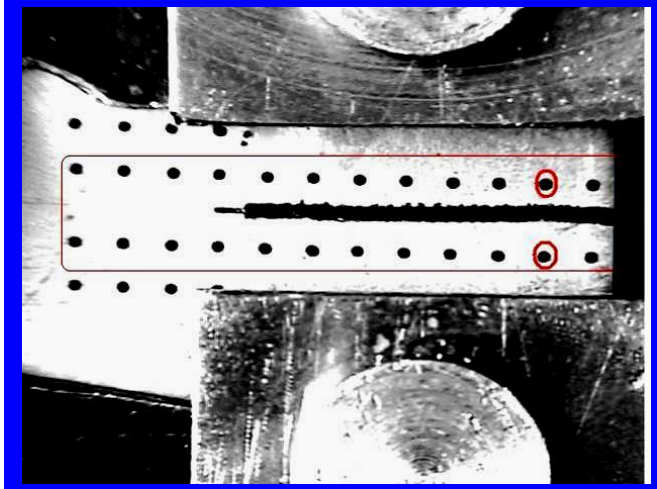

- Electrospark notch root R = 0.1 mm
- Fatigue precrack
- Grid for non contact displacement measuring – Videoextensometry

Kinetics of notch root deformation

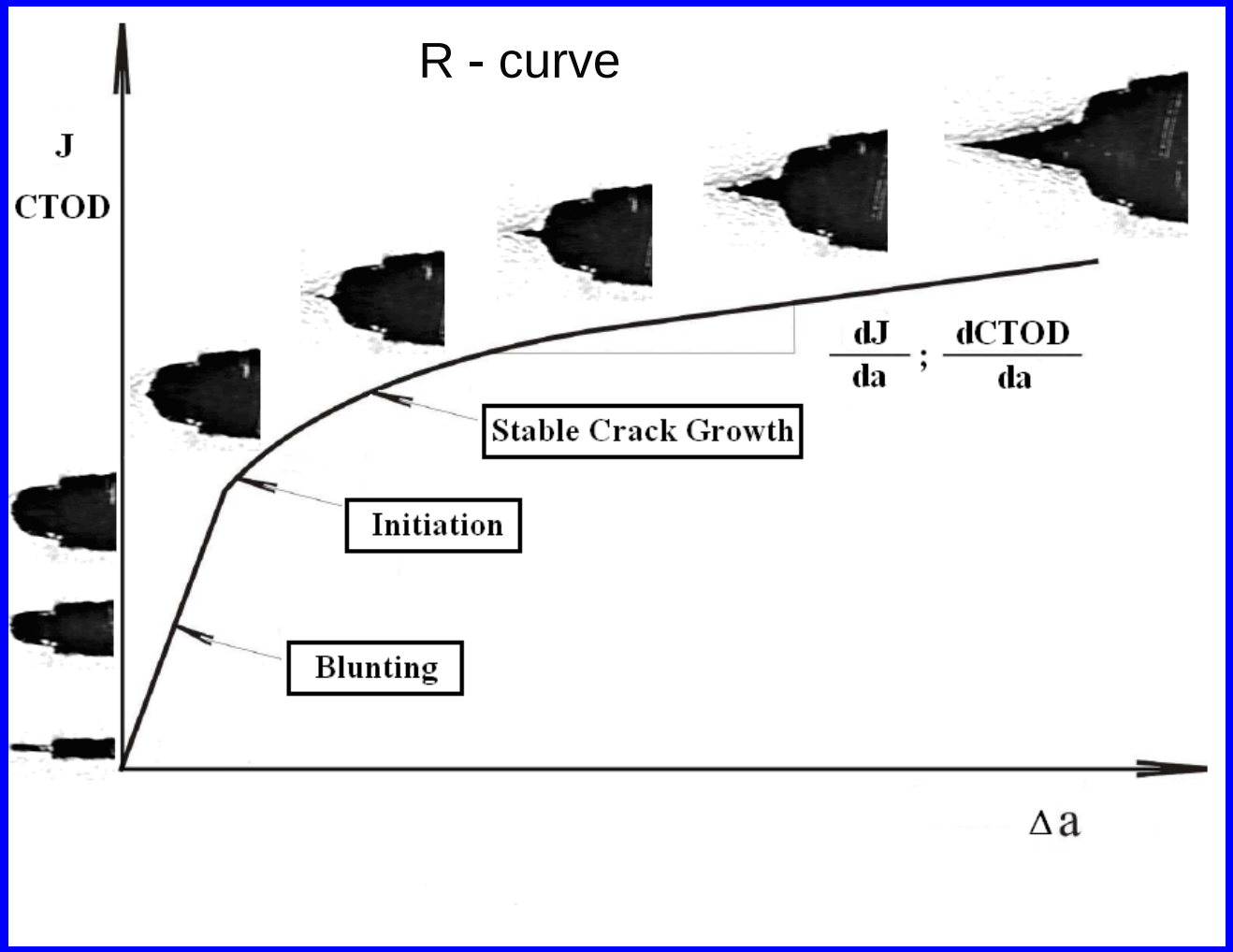

$$T = \frac{dJ}{da}\frac{E}{R_{em}^2}$$

$$R_{em} = \frac{(R_e + R_m)}{2}$$

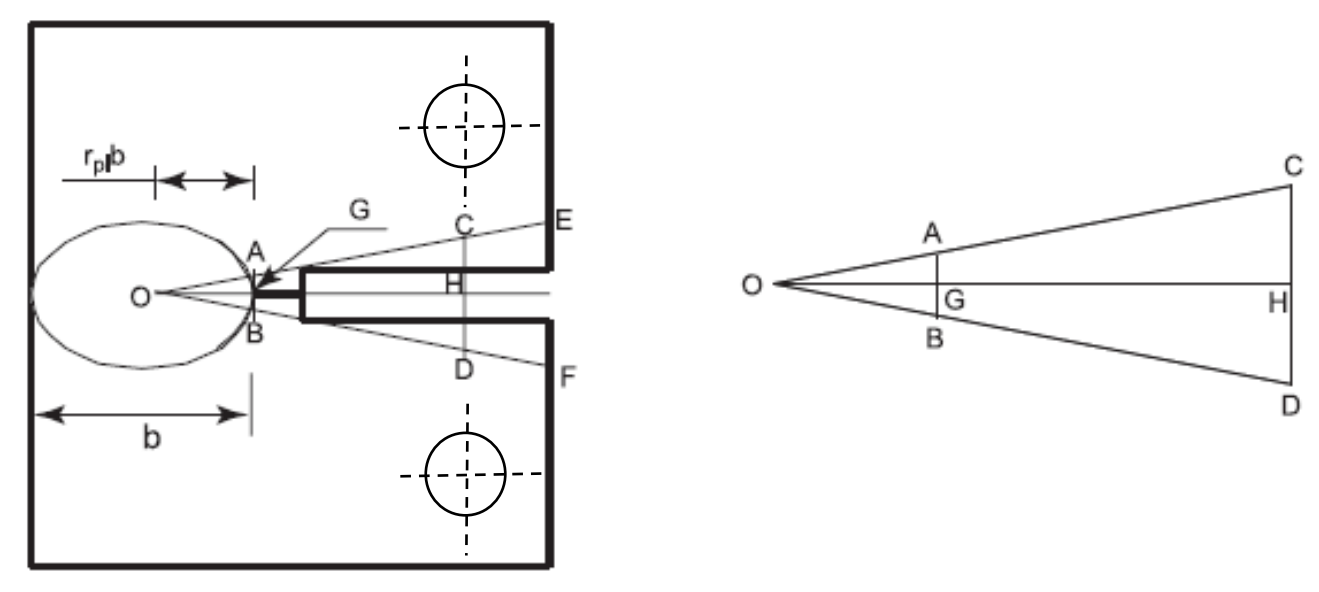

O = plastic hinge

$$\frac{AB}{CD} = \frac{OG}{OG + GH} \quad or \quad \frac{CTOD}{V} = \frac{r_{pl}b}{r_{pl}b + a_0}$$

$$CTOD = \frac{\left(r_{pl}(W - a_i) + \Delta a_i\right)V_c}{\left(r_{pl}(W - a_i) + a_i + z\right)}$$

$$n = \frac{r_{pl}}{b}$$

$$r_{pl} = 0{,}4(1 + \alpha_i)$$

$$\alpha_i = 2\left[\left(\frac{a_i}{W - a_i}\right)^2 + \left(\frac{a_i}{W - a_i}\right) + \frac{1}{2}\right]^{\frac{1}{2}} - 2\left[\frac{a_i}{W - a_i} + \frac{1}{2}\right]$$

Plastic hinge

n - changes during loading

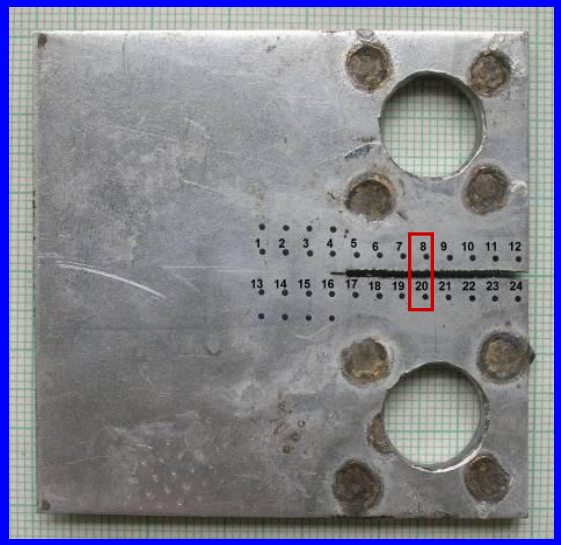

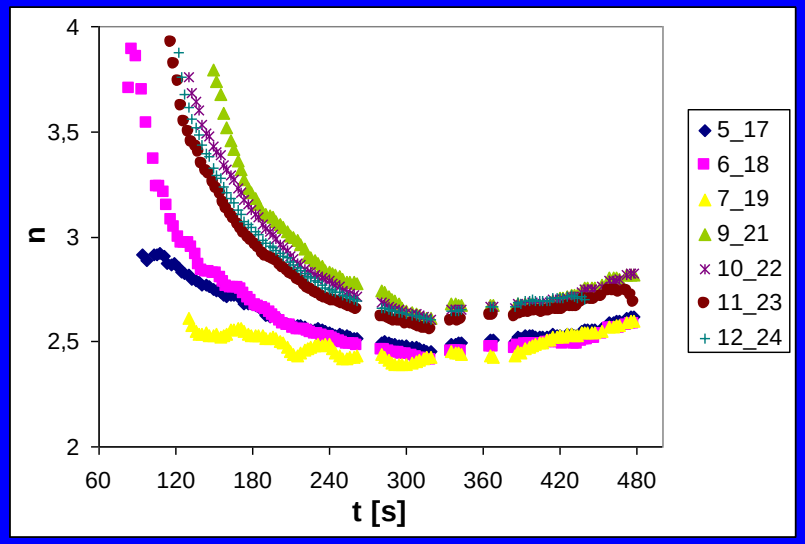

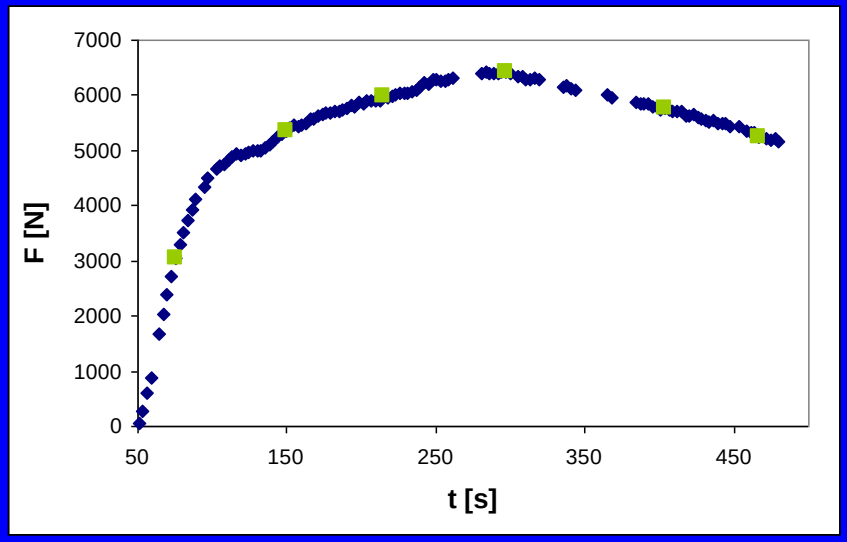

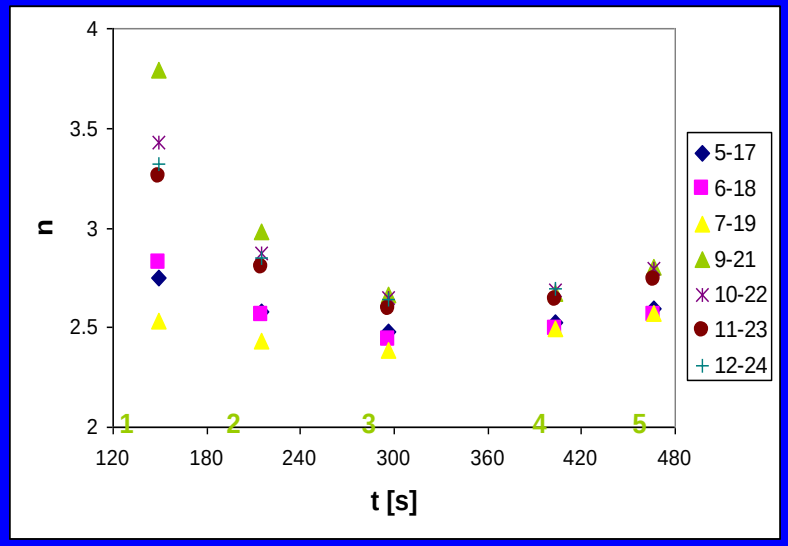

R-curves – 1.3 mm/min

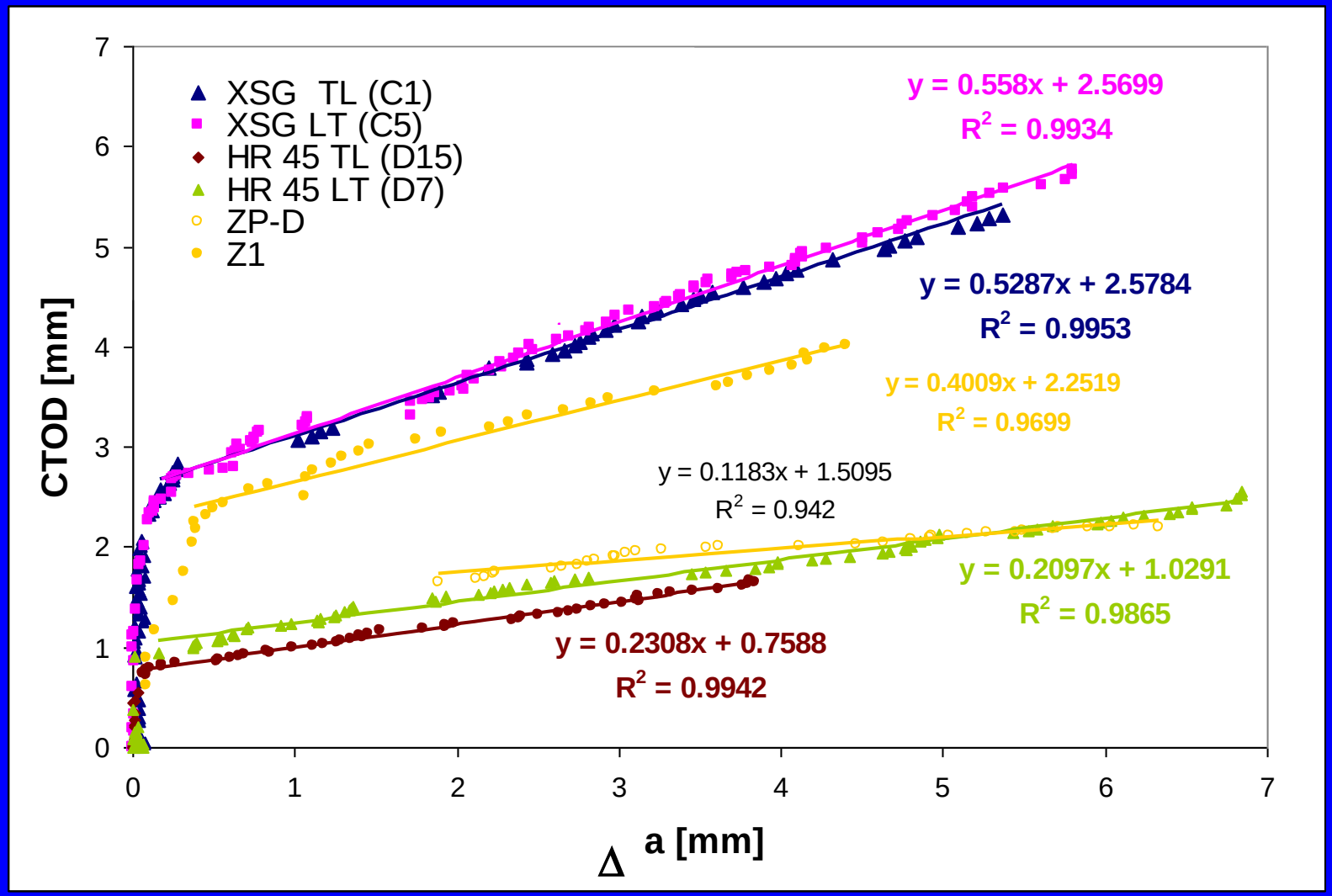

R-curves – 130 mm/min

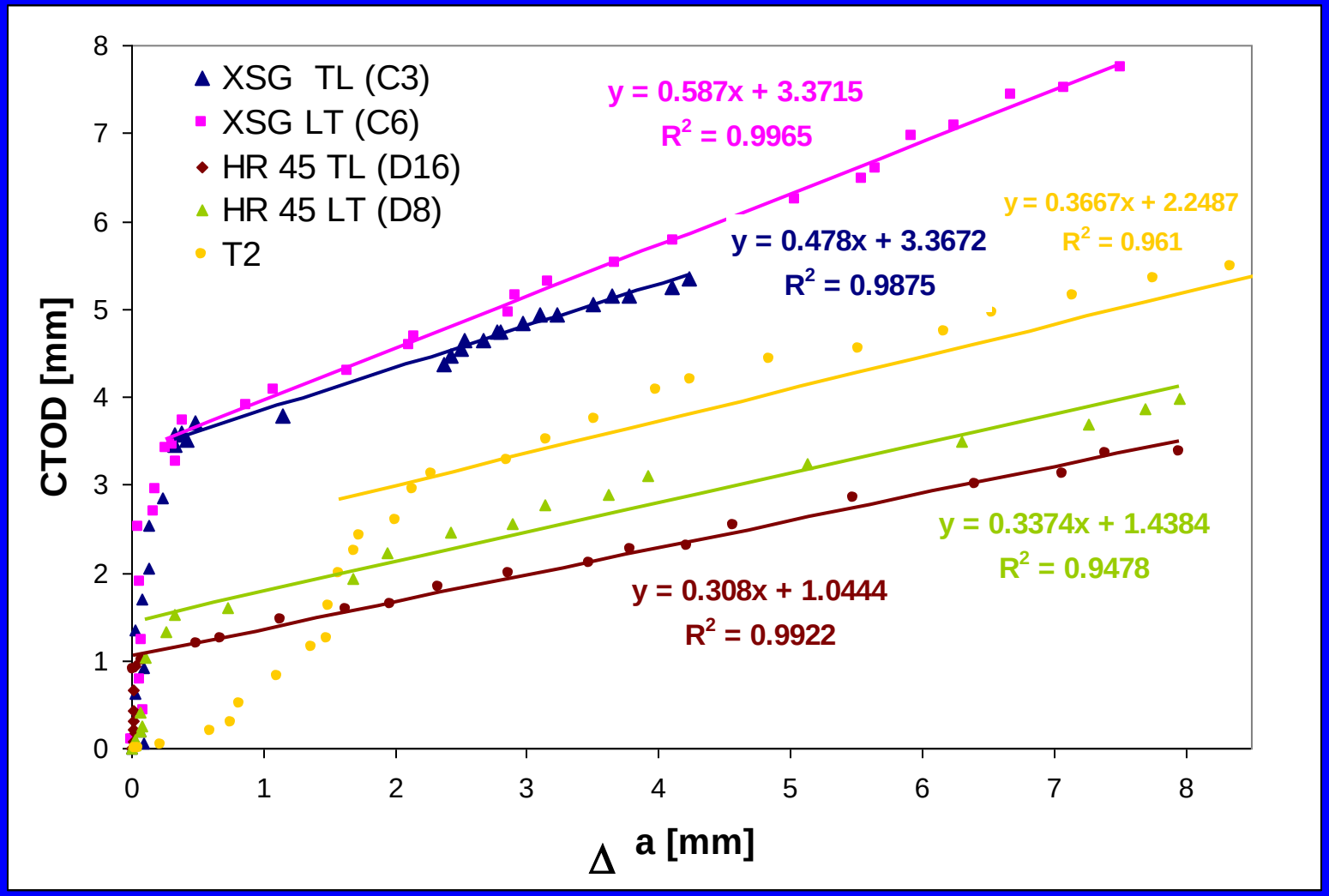

R-curves – fatigue (f), electrospark

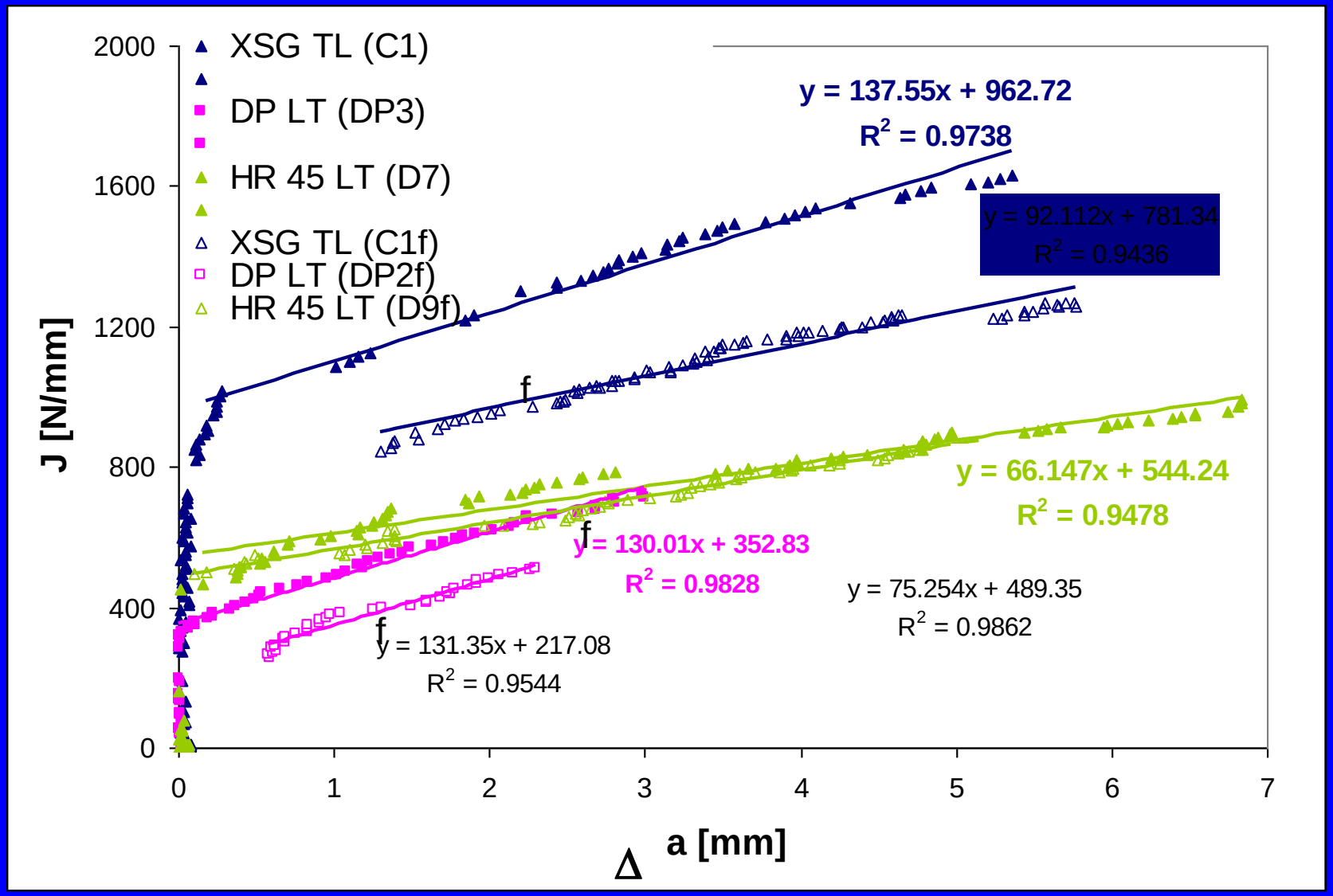

R-curves – fatigue (f), electrospark

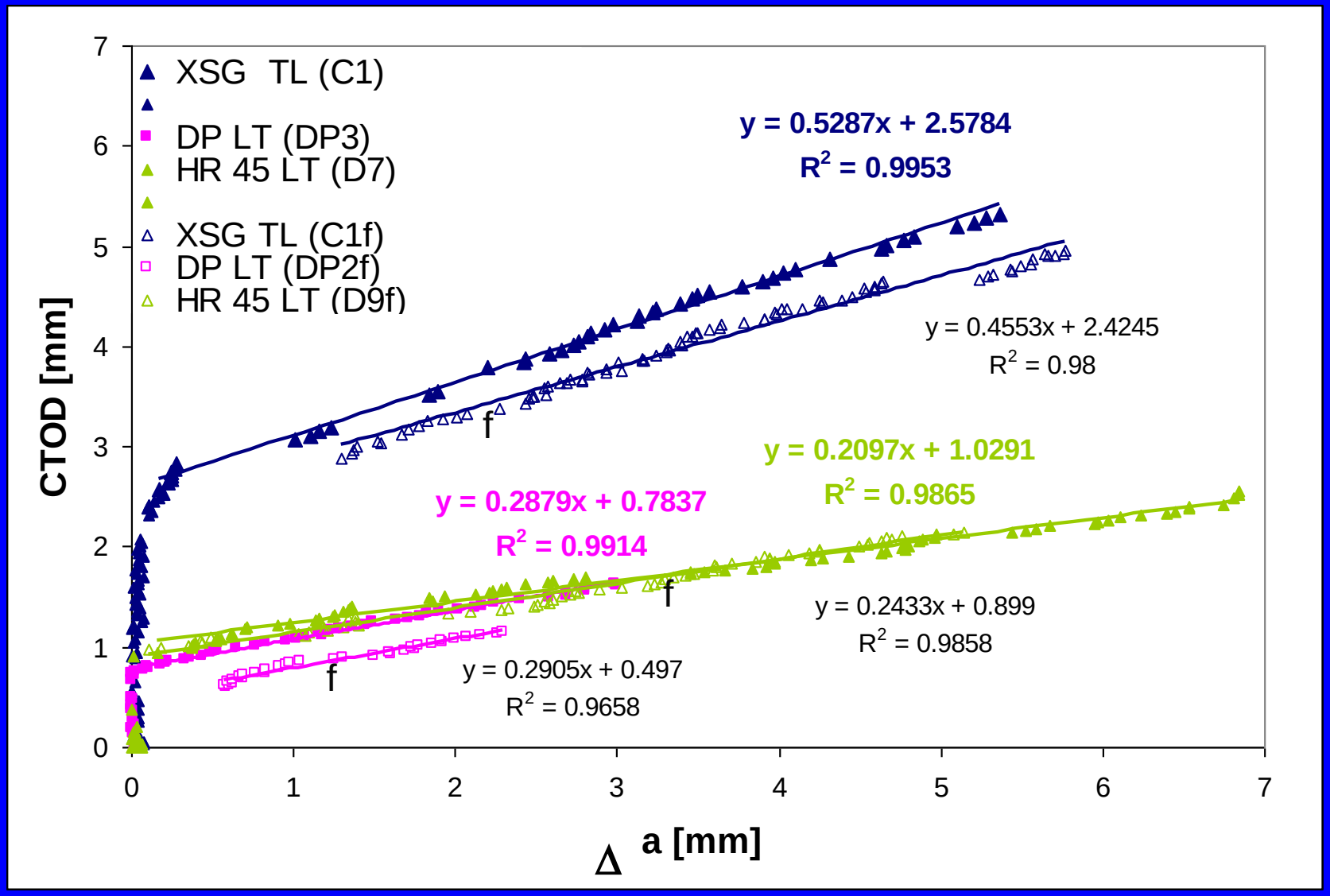

CT specimens with laser welds

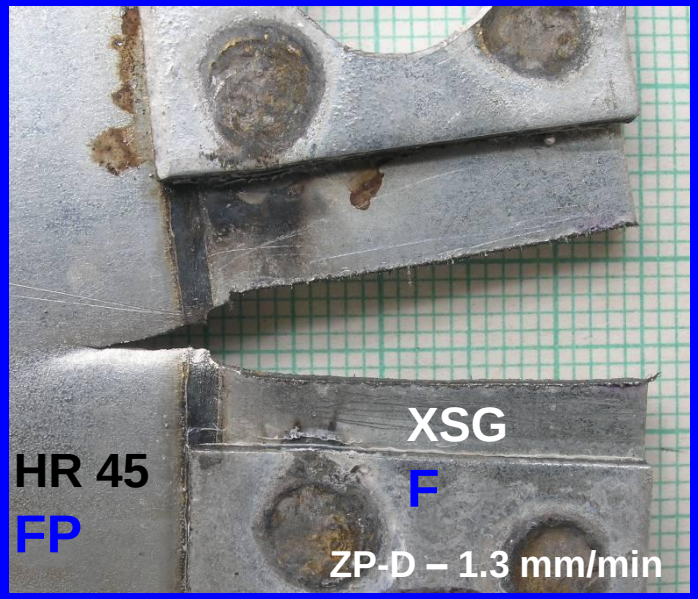

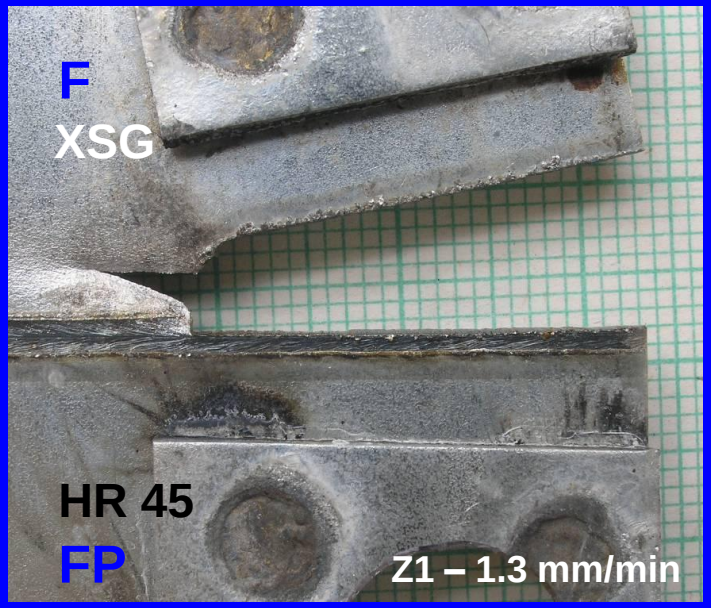

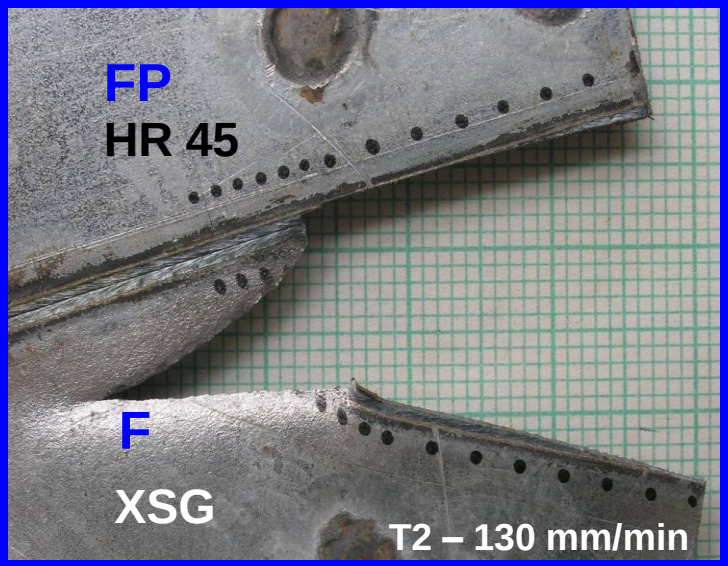

Stable crack growth resistance (130 mm/min)

Steel	Crack orientation	dCTOD/da	T
F (IF)	L - longitudinal	0.478	392
	T - transversal	0.587	419
FP	L	0.308	134
	T	0.337	206
T2	L weld (IF)	0.367	-

Steel sheets welded by laser beam

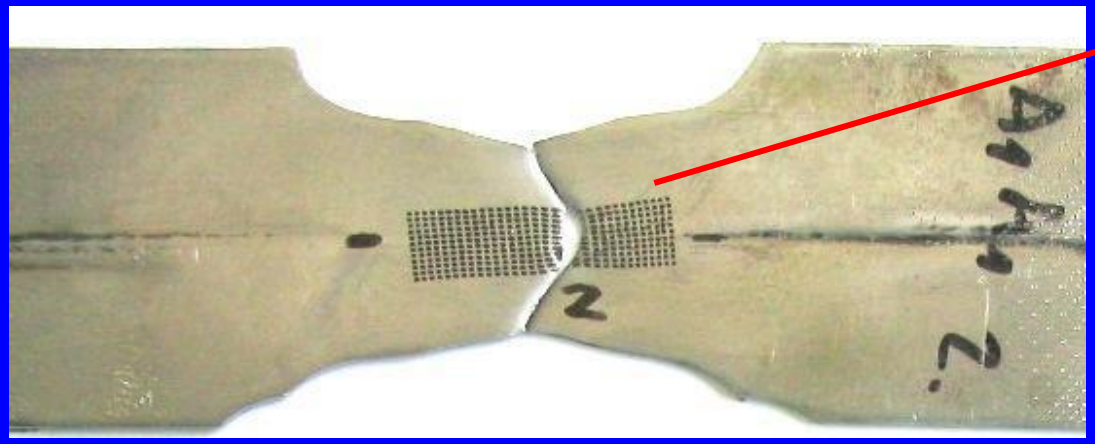

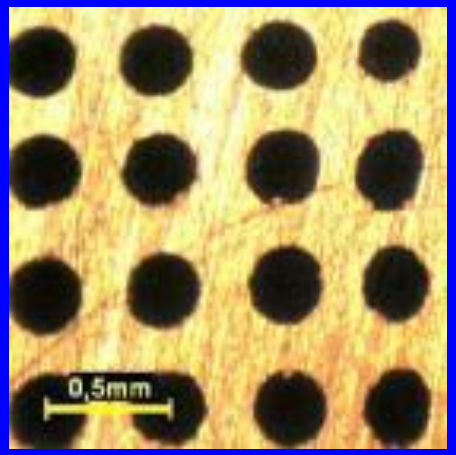

Numerical strain map

42,4	63,5	41,7	49,9	29,2	33,2
46,0	78,3	52,1	29,2	25,9	25,2
39,2	91,7	63,5	21,0	20,7	31,7
25,0	**95,8**	63,7	29,2	21,6	25,0
31,9	82,9	69,3	33,5	21,6	34,7
43,6	58,5	53,9	54,8	37,2	26,3
33,5	54,2	51,9	48,0	43,5	37,5
34,9	51,9	34,7	50,2	52,2	45,5
43,3	39,3	43,3	41,7	51,9	46,0
32,1	40,9	34,7	47,8	47,7	50,2
34,9	37,5	24,8	34,9	52,1	50,0

Strain maps of laser welded steel sheets

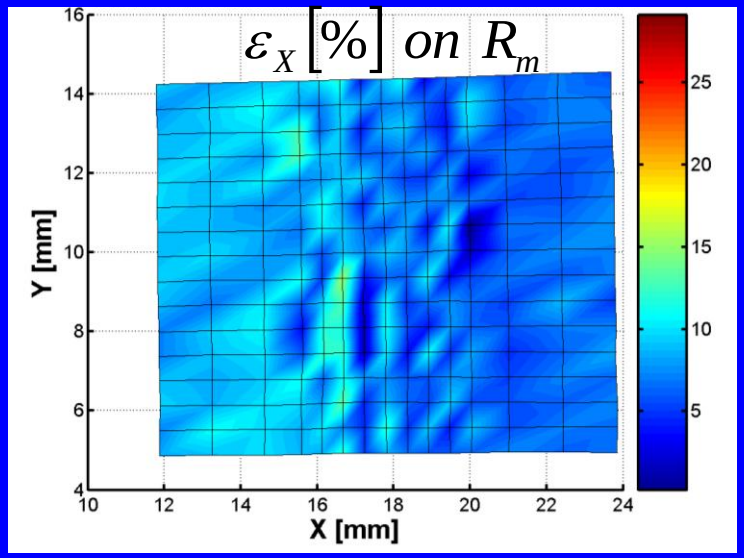

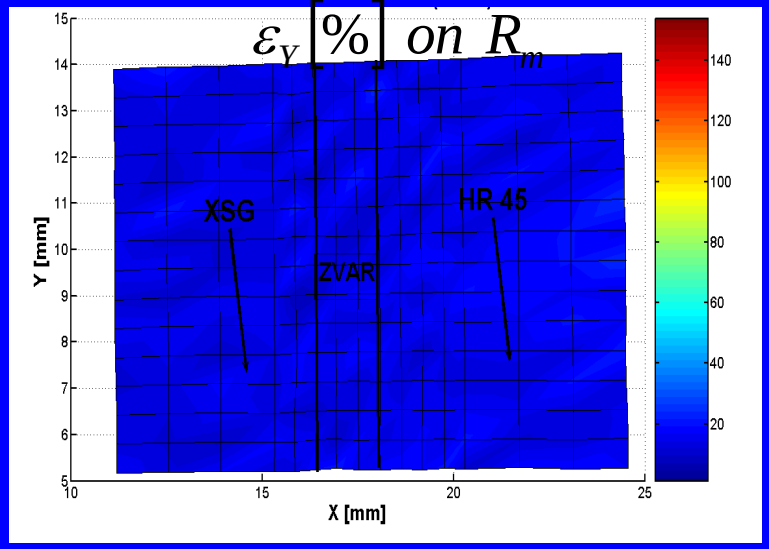

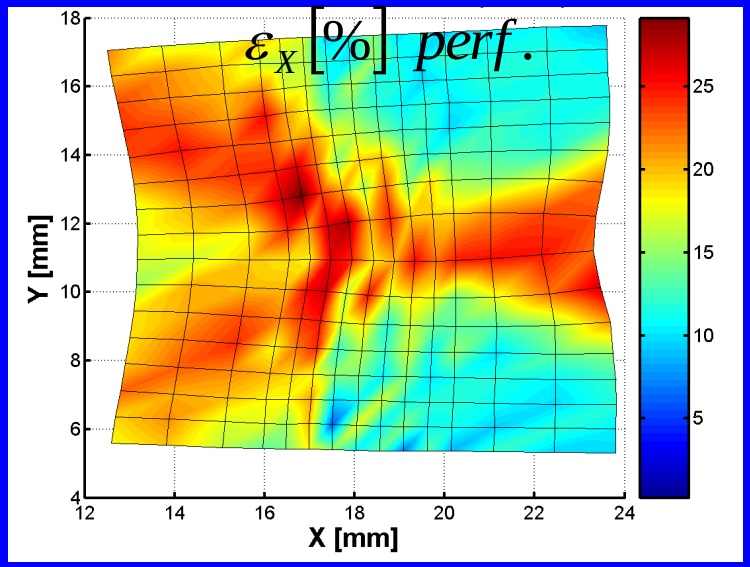

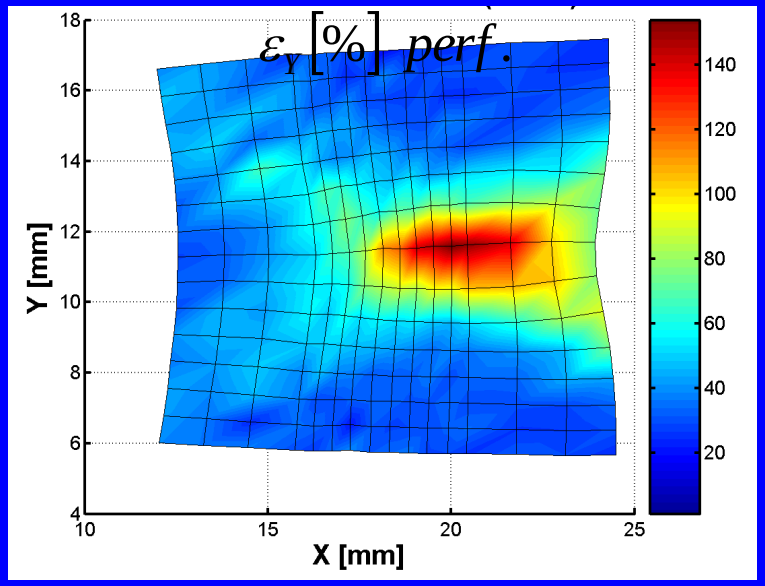

Elasticity limit – 2D

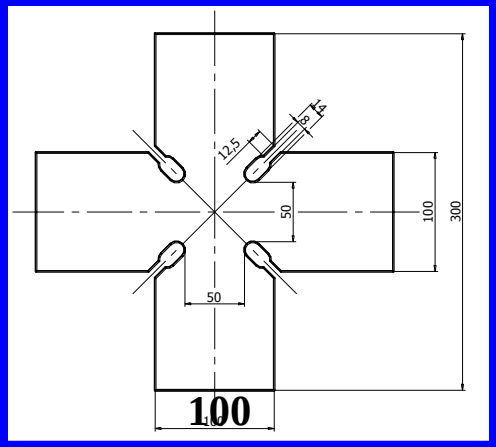

Krížová vzorka

1 CCD kamera
2 hydraulický valec

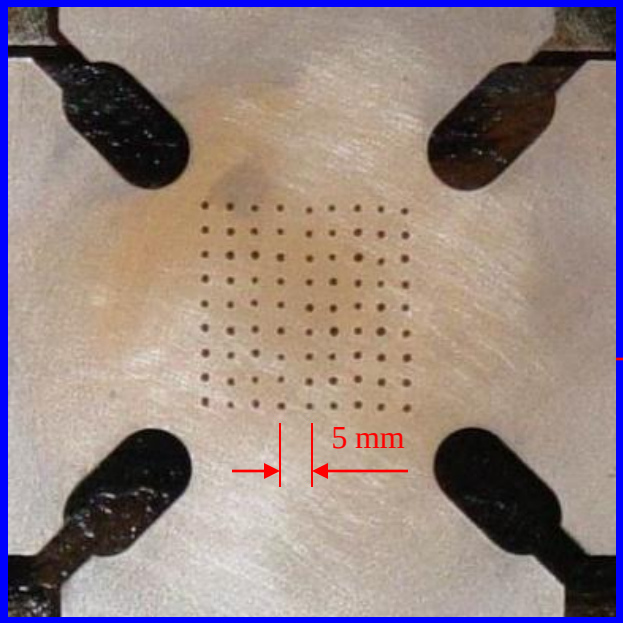

Rozmiestnenie bodov

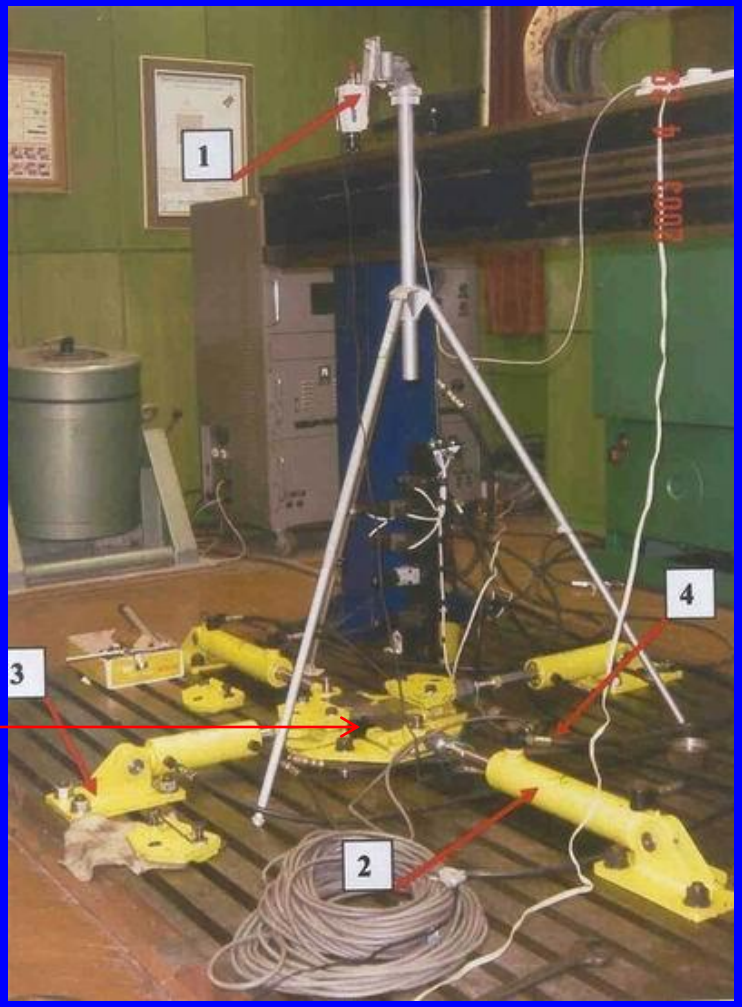

Elasticity limit – 2D

Displacement of 2 points

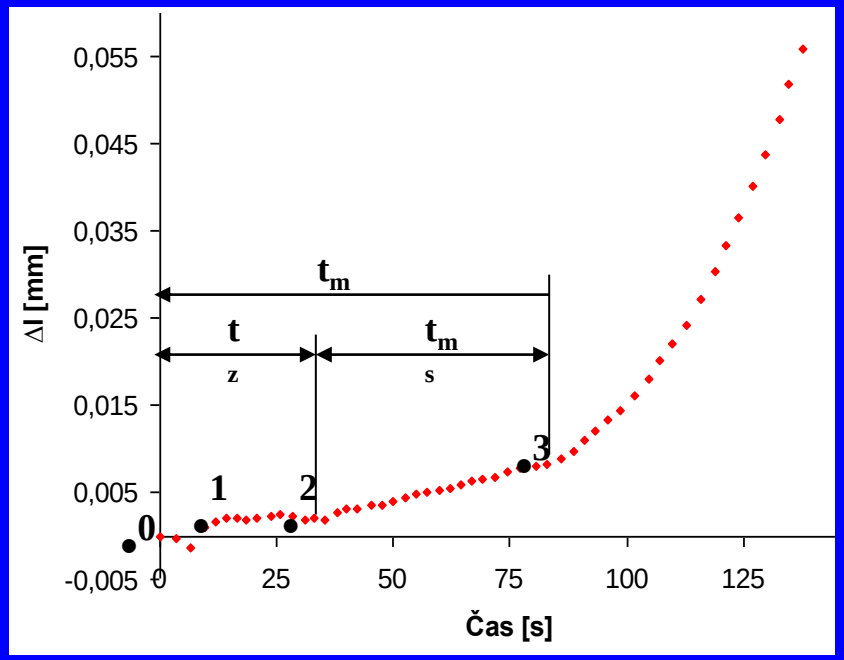

0-1 nábeh systému
1-2 ustálenie nuly
2-3 elastická oblasť
3 – začiatok plastickej deformácie

Deformačná mapa

Časy začiatku plastickej deformácie

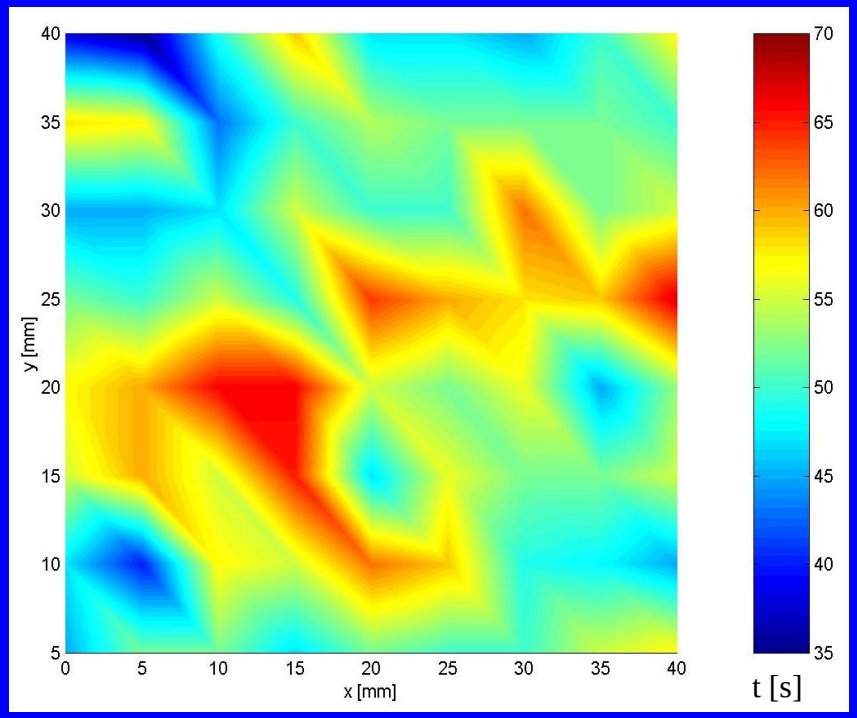

Elasticity limit – 2D

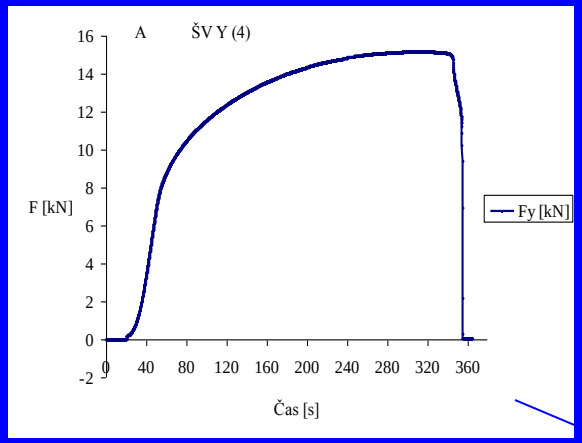

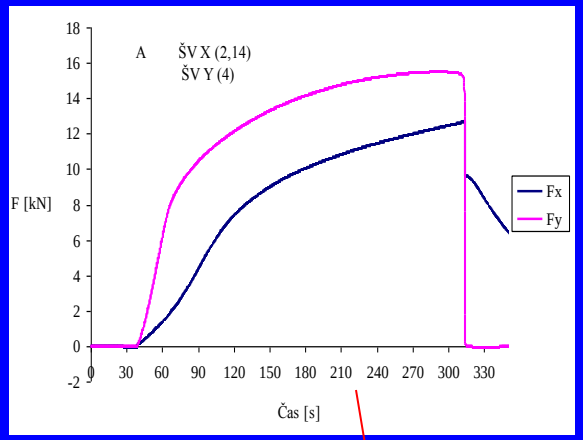

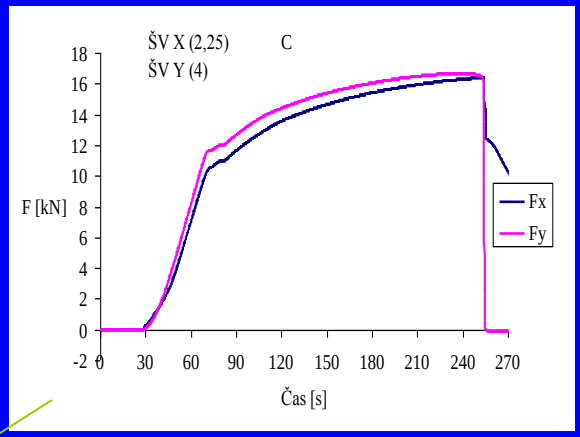

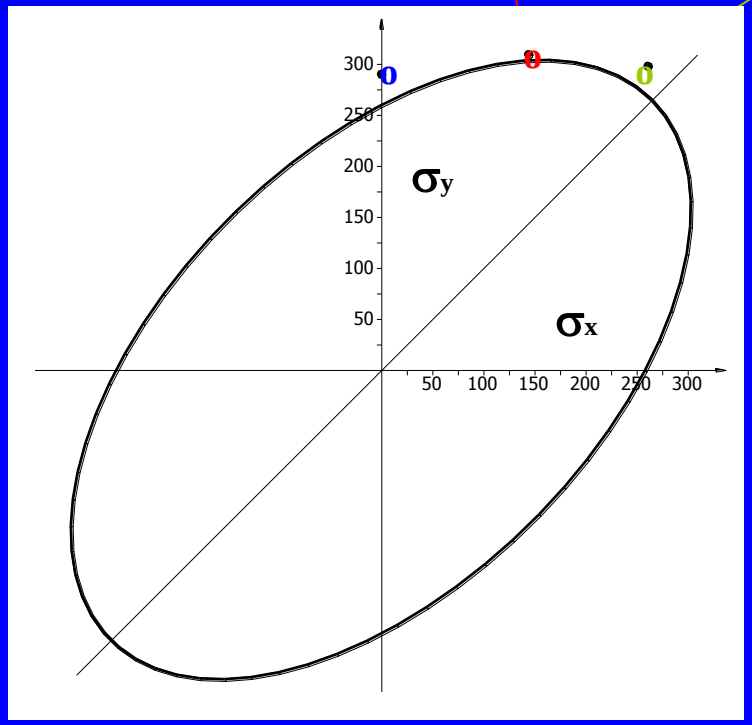

Plasticity curve

Fracture toughness of fibre reinforced concrete

3PB 100 x 100 x 300 mm

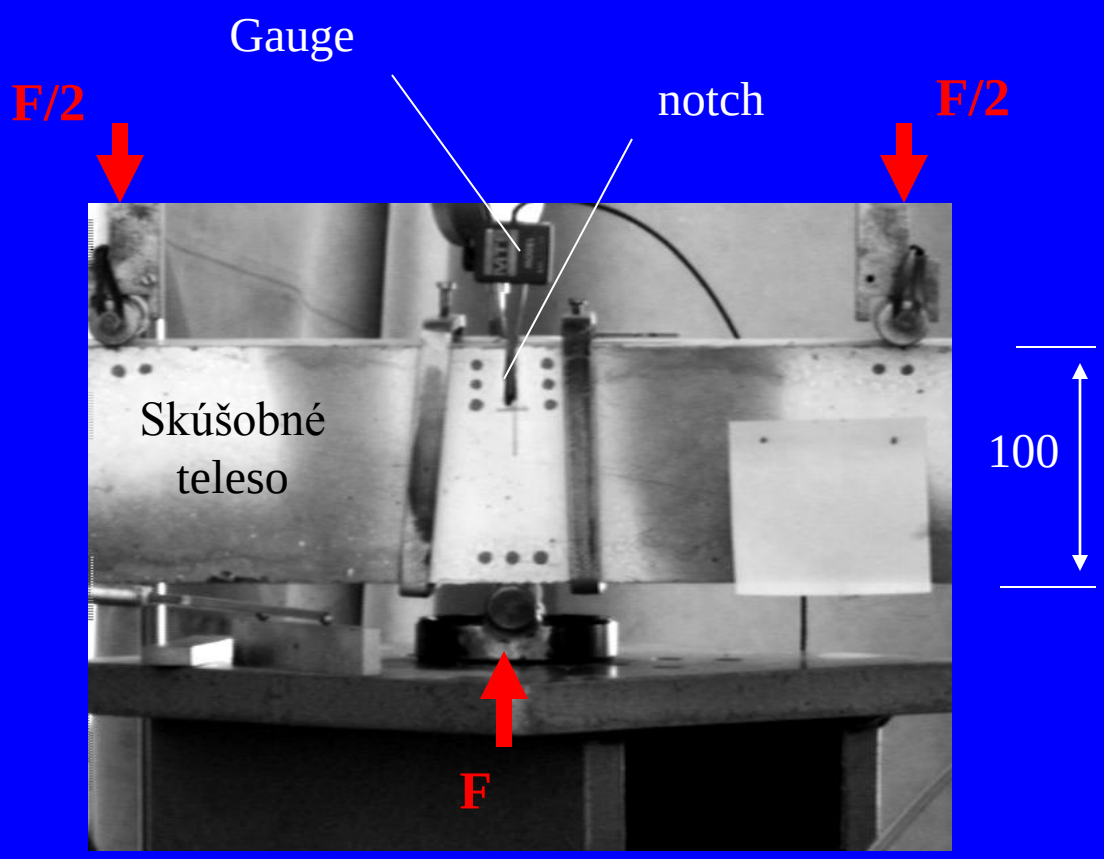

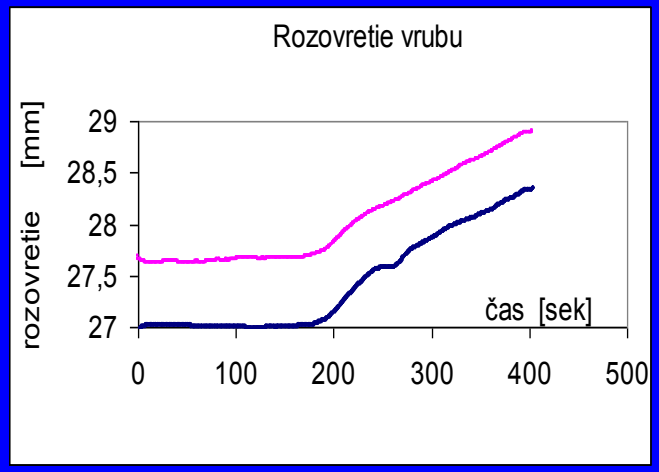

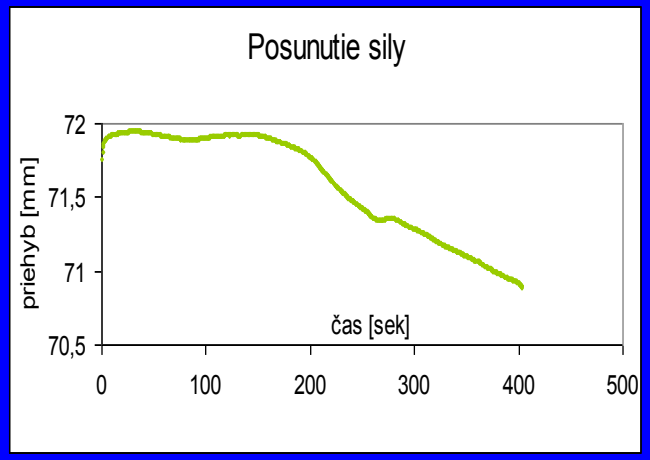

Videoextensometry – non contact displacement measuring

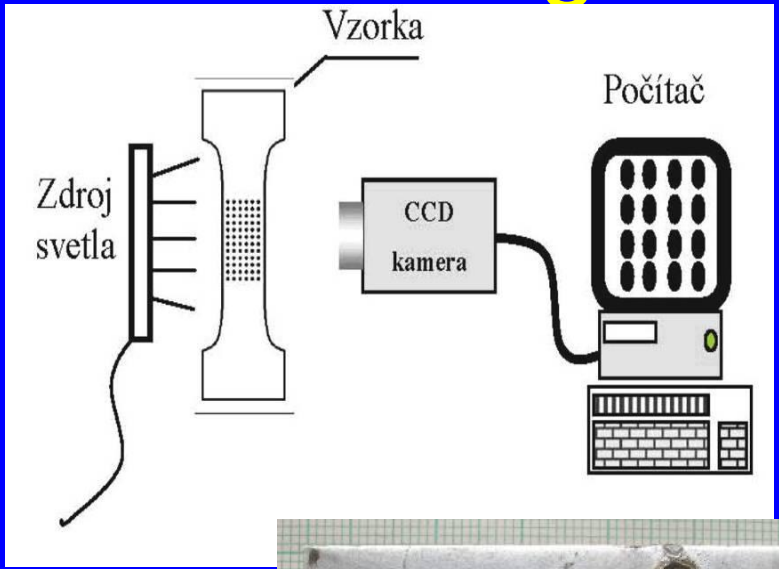

- Non-contact
- Output:

a) Data (x-, y- co-ordinates)
up to 10 Hz
(.dat)

b) Sequency of images during test
(.bmp)

Stable crack growth resistance (1.3 mm/min)

Steel	Crack orientation	dCTOD/da	T
F (IF)	L - longitudinal	0.529	569
	T - transversal	0.558	585
FP	L	0.231	114
	T	0.21	116
weld	L weld (IF)	0.401	-
weld (F → FP)	T weld	0.118	-

Stable crack growth:

Crack opening

Mode I...K_I

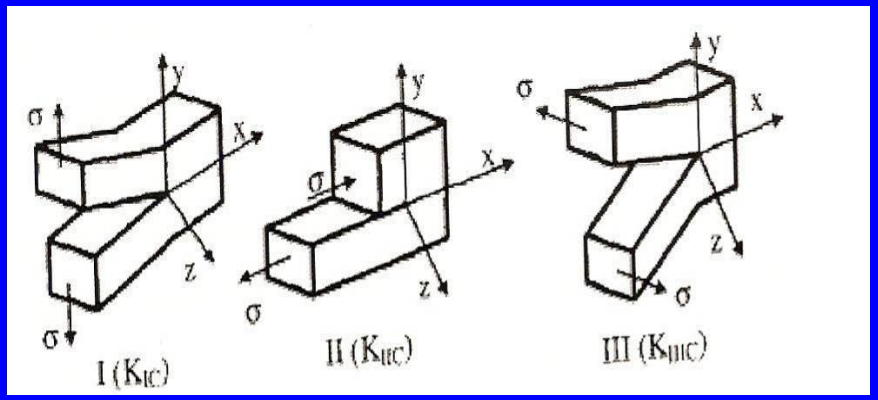

Mode III... K_{III}

Trousers test

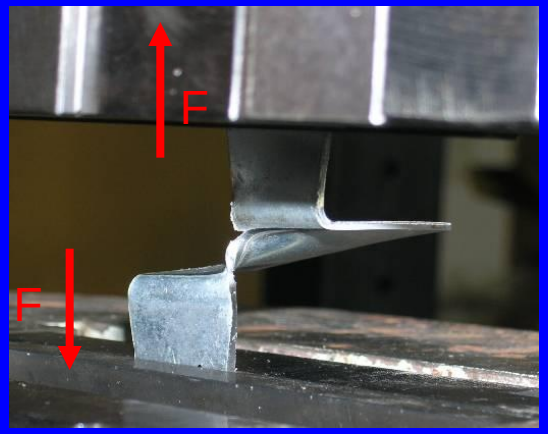

Optimization - CT specimen

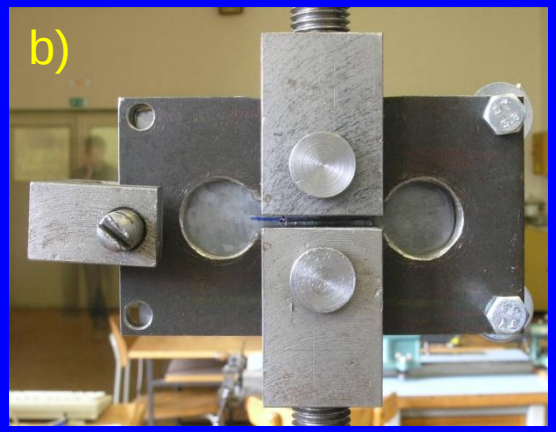

a) Buckling
b) Stiffening plates
c) Without buckling
d) Before loading
e) After loading

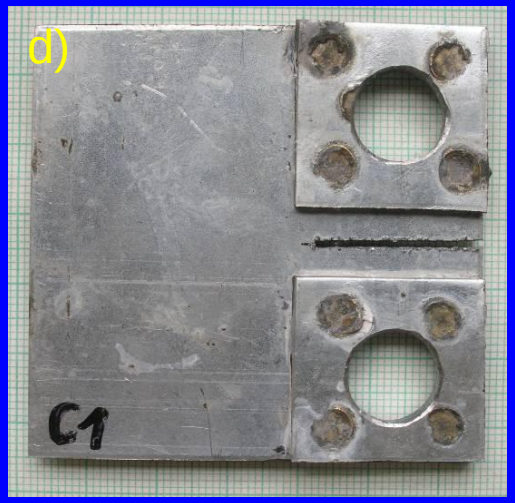

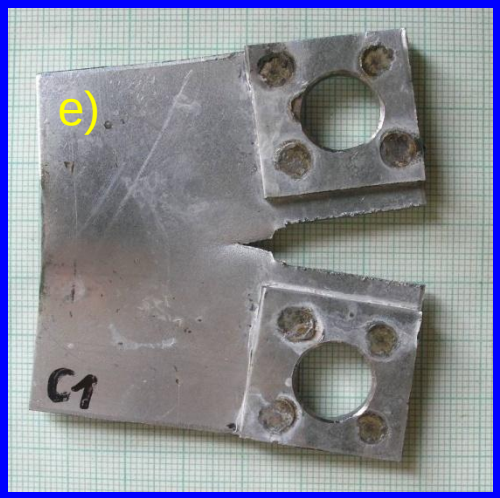

CT specimen

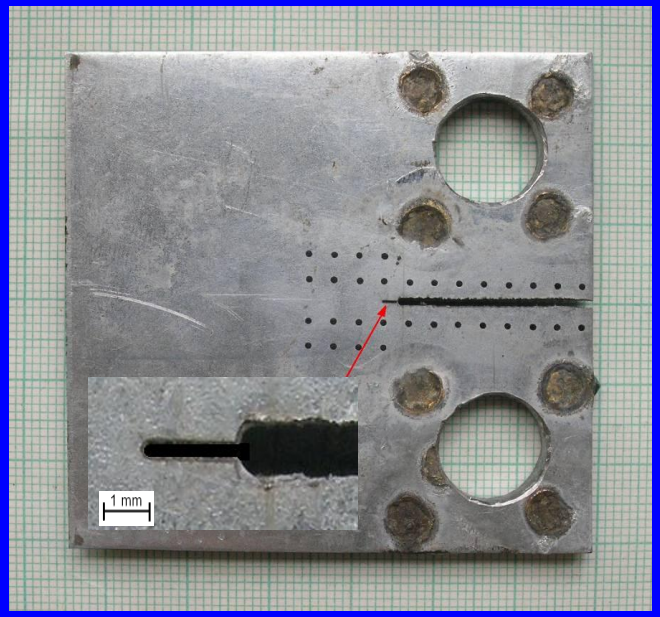

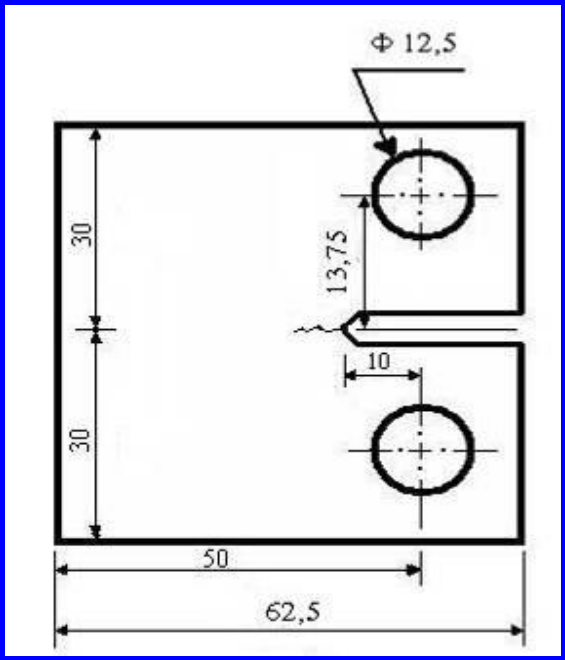

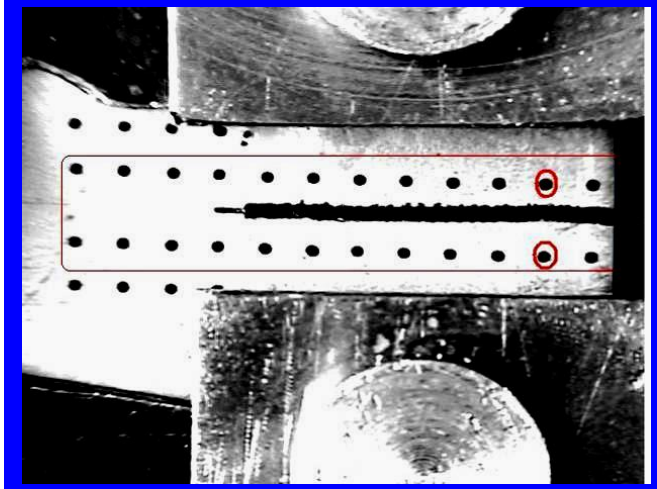

- Electrospark notch root R = 0.1 mm
- Fatigue precrack
- Grid for non contact displacement measuring – Videoextensometry

Steel sheet properties

Mechanical properties

Steel	R_e [MPa]	R_m [MPa]	A [%]	Thickness [mm]
F (IF)	182	300	45	1.95
FP	382	493	25	1.8
DP	357	580	25	1.6

Chemical composition in [%]

Steel	C	Mn	S	P	Si	Al	Nb	V	Ti
F (IF)	0.0013	0.082	0.01	0.011	0.006	0.055	0.001	0.002	0.04
FP	0.16	0.65	0.004	0.013	0.010	0.035	0.001	0.002	0.01
DP	0.072	1.807	0.006	0.017	0.010		0.002	0.003	0.001

Microstructure

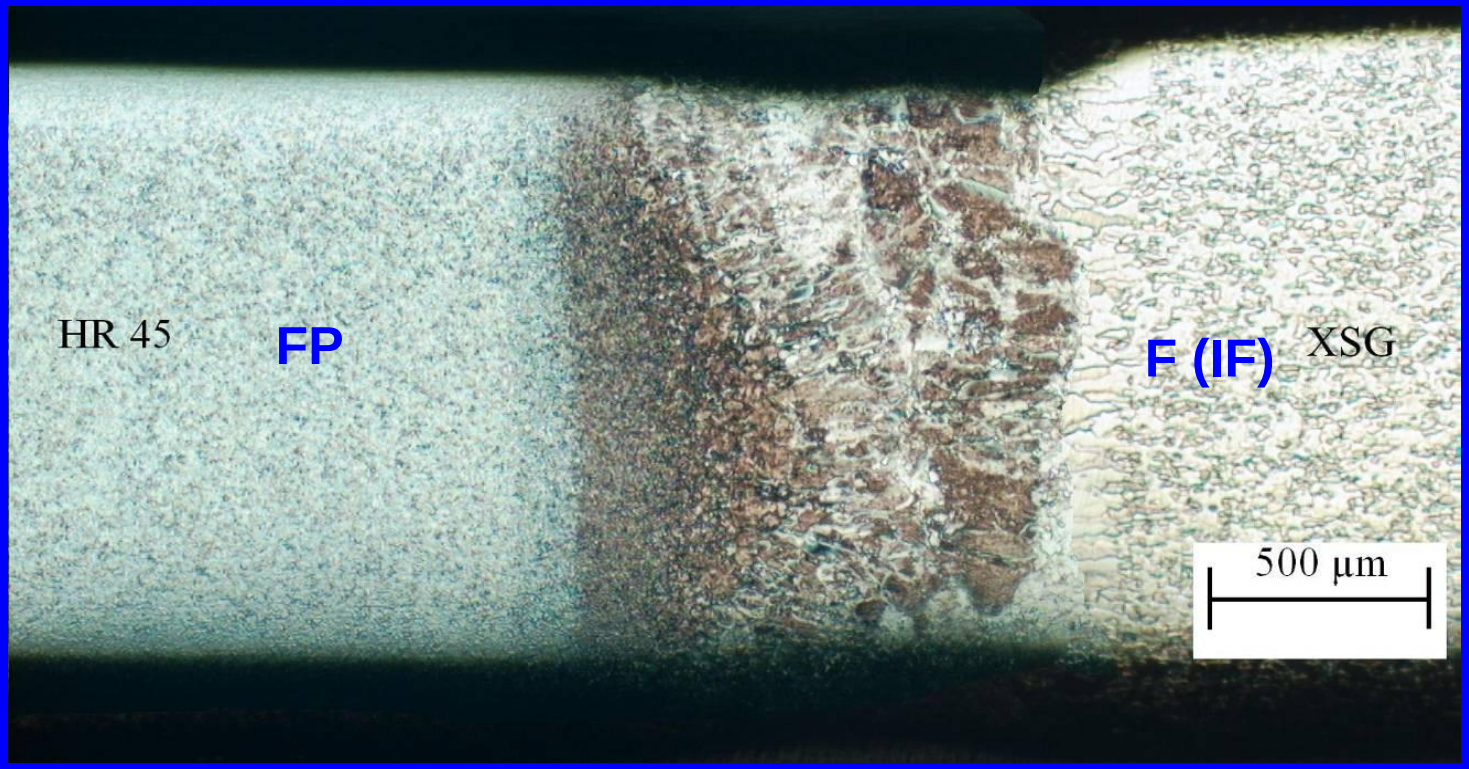

DP = (dual phase) FM

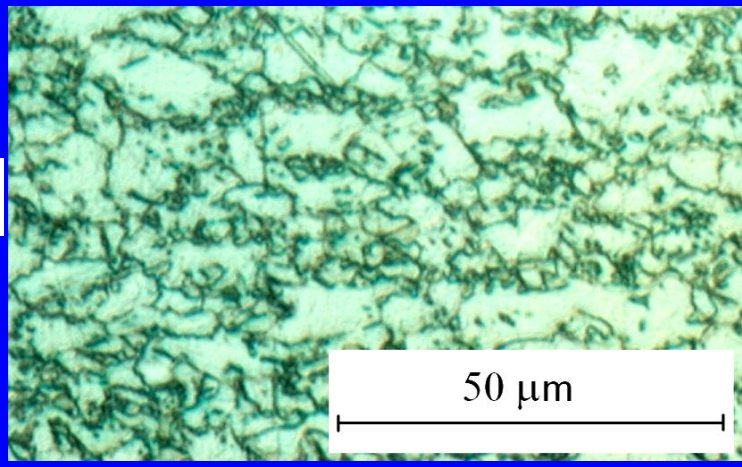

POROVNANIE DEFORMAČNÝCH CHARAKTERISTÍK OCEĽOVÝCH PLECHOV MERANÝCH V LOKÁLNYCH A GLOBÁLNYCH OBLASTIACH PRI STATICKOM ZAŤAŽENÍ POUŽITÍM VIDEOEXTENZOMETRIE

Experimentálna časť

1. Experimentálny materiál

- 2 materiály rovnakej akosti (OK, NOK) – hlbokoťažná oceľ (R_e=170-290 MPa, R_m=240-380 MPa), t = 3 mm
- 3 skúšobné vzorky z každého materiálu rozmerov 20x80 mm
- vybrané vzorky v smere kolmom na smer valcovania
- 2 spôsoby nanášania bodiek (globálna a lokálna oblasť)

Obr 1 Kryt kompresora s trhlinou

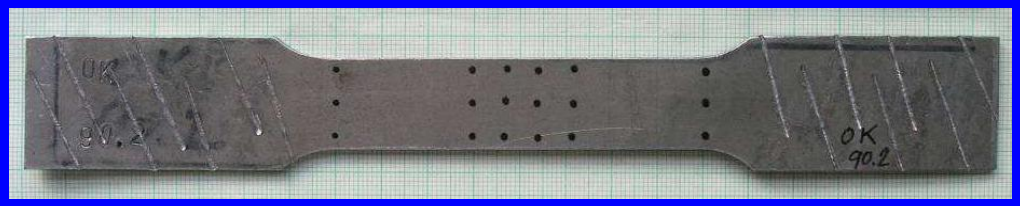

Obr 2 Vzorka s nanesenými kontrastnými bodkami, vzdialenosť bodiek 7 mm – globálne meranie

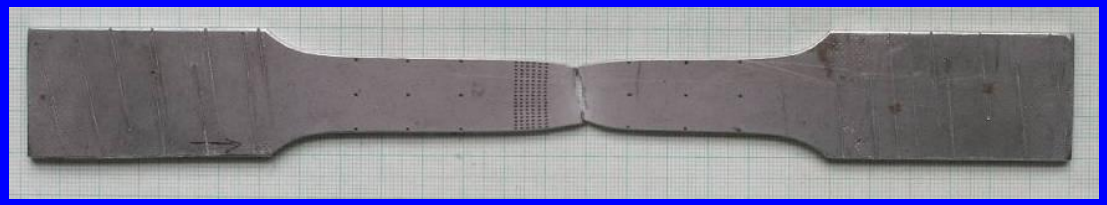

Obr 3 Vzorka s nanesenými kontrastnými bodkami, vzdialenosť bodiek 1 mm – lokálne meranie

1. Metalografická analýza

OK

perlit NOK

Obr 5 Mikroštruktúra ocelí

OK - feritická štruktúra

NOK - pozorovaný malý podiel perlitu

2. Statická skúška v ťahu

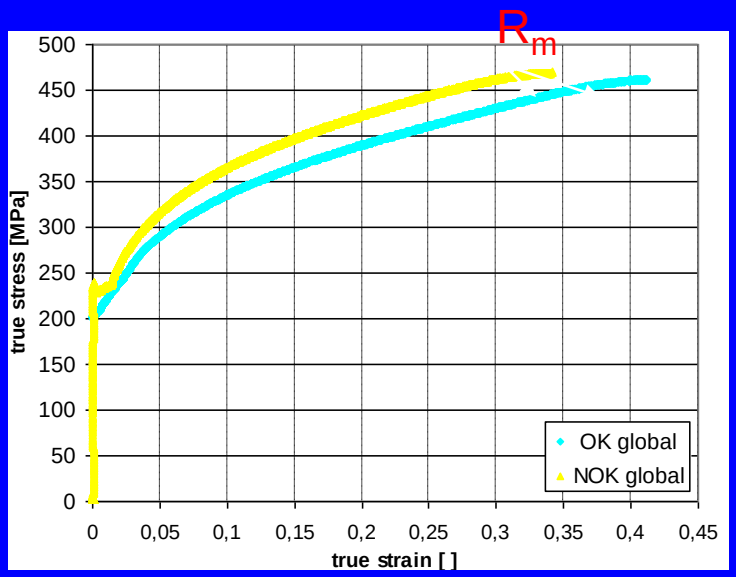

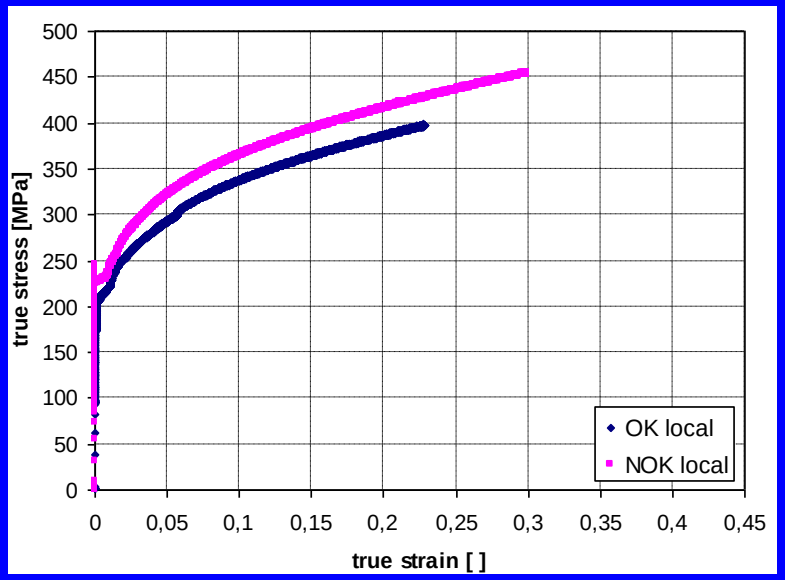

a) globálna oblasť vyhodnocovania

b) lokálna oblasť vyhodnocovania

Diagram skutočné napätie – skutočná deformácia do R_m

Mechanické vlastnosti skúmaných ocelí

Označenie ocelí	$R_{p0,2}$ [MPa]	R_{eH} [MPa]	R_m [MPa]	A_{80} [%]
OK	199		315	41
NOK		238	341	34

NOK - výrazná medza sklzu

- R_e, $R_m \uparrow$ o 30 MPa

Exponent bol vyhodnocovaný z lineárnej oblasti diagramu σ-φ v log súradniciach na úseku φ = 0,05

Z týchto úsekov bol zostavený priebeh exponentu

- priebeh je vykreslený od R_e – R_m
- tesne pred R_m začína n rapídne klesať
- rozdiel aj medzi lokálnou a globálnou oblasťou vyhodnocovania, lokálna udáva nižšie hodnoty n

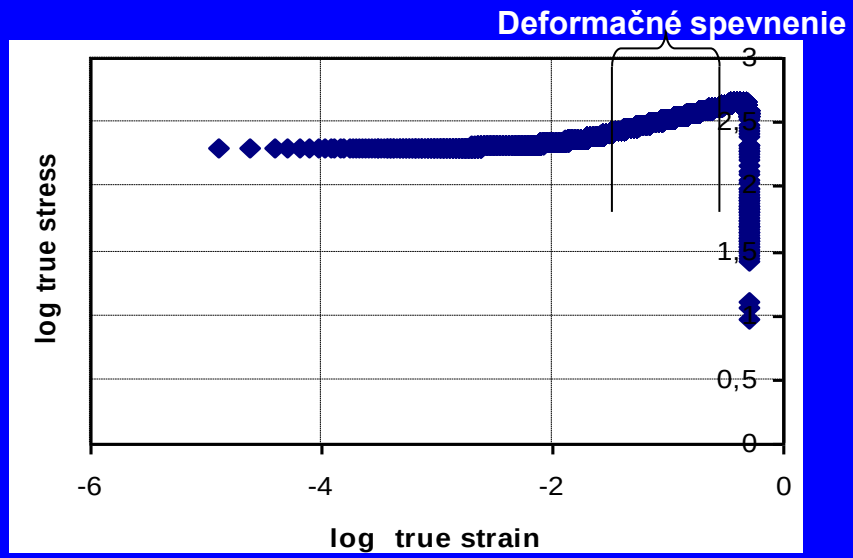

Diagram log σ – log φ

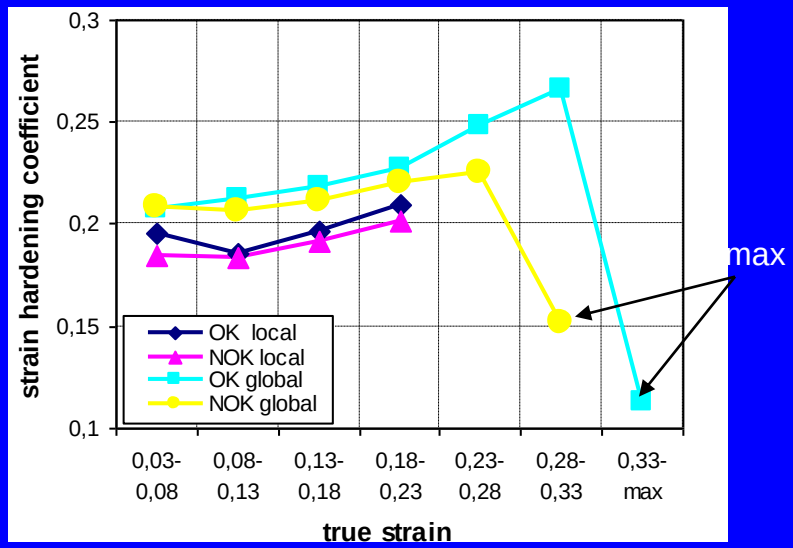

Priebeh exponentu deformačného spevnenia v závislosti od skutočnej deformácie

Koeficient normálovej anizotropie

- pomer šírkovej a hrúbkovej deformácie
- ideálny prípad pre plechy určené na hlboké ťahanie

nastane, ak r je čo najvyšší a $\Delta r = 0$

$$r = \frac{\ln \frac{b_0}{b_1}}{\ln \frac{h_0}{h_1}} = \frac{\ln \frac{b_0}{b_1}}{\ln \frac{l_1 b_1}{l_0 b_0}}$$

Kde: l_0, b_0, h_0 – dĺžka a šírka pred deformáciou [mm]
l_1, b_1, h_1 – dĺžka a šírka po deformácii [mm]

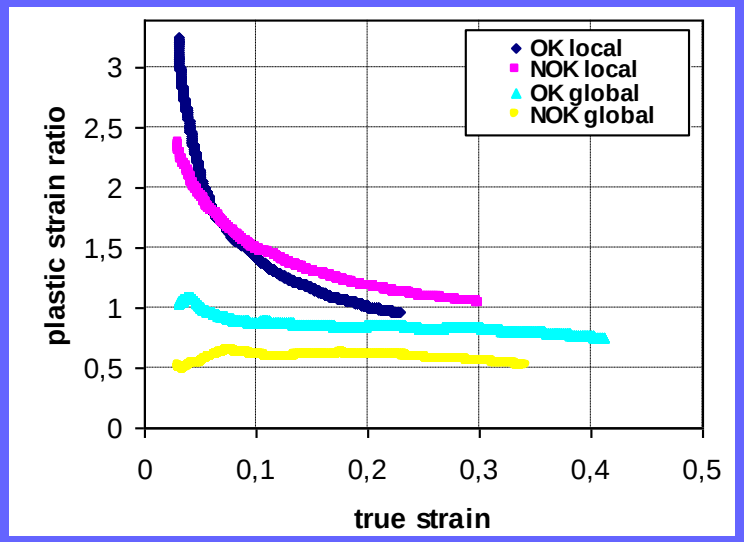

Obr 9 Priebeh koeficientu normálovej anizotropie v závislosti od skutočnej deformácie

Lokálna oblasť vyhodnocovania – hodnoty silne závislé od deformácie => neustálené

V oboch prípadoch – koeficient má klesajúci trend